ADVANCED FUNCTIONAL MATERIALS
www.afm-journal.de

Advances in Micro/Nanofiber-Based Porous Materials for High-Performance Thermal Insulation

Xiaobao Gong, Shuo Shi, Jing Yin, Rong Liu, Jianming Chen, and Xungai Wang**

Thermal insulation materials serve as critical components in daily life and industrial processes that protect humans against the cold environment, minimize energy consumption, and promote sustainable development. Emerging micro/nanofiber-based porous thermal insulation materials, exhibiting much lower thermal conductivity than the commercial mainstream materials, have gained widespread attention in recent years. Herein, a comprehensive review is presented on the advancements in micro/nanofiber thermal insulation materials, focusing on structural designs, fabrication techniques, and applications. This review starts with the fundamental heat transfer mechanisms inherent in porous thermal insulation materials. Then, a detailed discussion of the structural design of micro/nanofiber thermal insulation materials is given, ranging from the 2D fibrous membranes/textiles to the newly developed 3D sponges/aerogels. Furthermore, the representative applications of the micro/nanofiber thermal insulation materials are highlighted, in areas including personal protection equipment, aerospace, automobile industry, and the building sector. Finally, the review outlines the existing challenges and future research directions of the micro/nanofiber thermal insulation materials, such as new thermal insulation mechanisms, long-term structural stability, and sustainable fabrication technologies. This review is expected to advance the diversification of thermal insulation materials and significantly contribute to the development of sophisticated thermal management systems.

1. Introduction

With the accelerating development of heavy industry and urbanization, the increased energy consumption has contributed to the accelerating depletion of fossil fuels and escalating greenhouse gas emissions.[1,2] Recent statistics revealed that the temperature control systems of the building consume nearly 30% of global energy resources while contributing 10% of anthropogenic CO_2 emissions.[3–5] To address the energy and environmental crisis, a global consensus has been reached on accelerating the development of sustainable energy alternatives while systematically improving the operational efficiency of traditional equipment.[6,7] Although renewable energy sources, such as solar, wind, and biomass energy, currently supply 14% of global demand, technological barriers, including inefficient energy conversion in photovoltaics and costly storage solutions, still exist.[8] Thermal insulation materials, which reduce heat transfer through engineered thermal resistance, are crucial to improving energy efficiency in almost all energy conversion and storage processes.[9–11] Among the presently available thermal insulation materials, fiber materials have served as primary thermal insulators throughout human history due to their favorable balance of comfort, manufacturability, and economic viability.[12]

In the realm of fiber thermal insulation, the market presents two primary categories: natural fiber materials and chemical fiber materials.[13,14] Natural thermal insulation materials, such as cotton, ceiba, wool, and down, have been widely employed for centuries, primarily due to their abundant availability.[15–17] Despite their historical prevalence, these natural fiber materials face inherent limitations. Their thermal insulation capacity is constrained by the large fiber diameters (usually >15 µm) and hygroscopic properties, leading to relatively high thermal conductivity. Furthermore, natural fiber's vulnerability to pest infestation fundamentally compromises material integrity, significantly accelerating performance degradation over time.[18] In contrast, chemical fibers have been widely used in the field of thermal insulation materials attributed to their moisture-proof, cost-effectiveness, and satisfactory application performance. Moreover, the chemical fibers could introduce engineered architectures such as pores and 3D crimps to enhance thermal insulation.[19–21] As a typical example, industrial-grade polyester fiberfill exemplifies advanced thermal engineering with low thermal conductivity (28.9 $mW\,m^{-1}\,K^{-1}$), which represents 20% improvement in thermal resistance compared to conventional cotton fiberfill

X. Gong, S. Shi, J. Yin, R. Liu, J. Chen, X. Wang
Joint Research Centre for Fiber Innovations and Renewable Materials
School of Fashion and Textiles
The Hong Kong Polytechnic University
Kowloon, Hong Kong, China
E-mail: jianming.chen@polyu.edu.hk; xungai.wang@polyu.edu.hk

The ORCID identification number(s) for the author(s) of this article can be found under https://doi.org/10.1002/adfm.202509492

DOI: 10.1002/adfm.202509492

(38.2 mW m^{-1} K^{-1}).[22] Although chemical fibers present comprehensive performance advantages, the challenges remain. Micrometer-scale fiber diameters (>10 µm) fundamentally restrict air entrapment efficiency, while manufacturing constraints hinder further reductions in material density and thermal conductivity.

In recent times, emerging micro/nanofiber technologies have presented revolutionary solutions to develop high-performance thermal insulation materials.[23–25] By precisely controlling fiber dimensions at submicron scales (diameters ranging from tens of nanometers to tens of micrometers), researchers have achieved optimized air/solid matrix configurations that simultaneously minimize heat transfer and convective losses.[26,27] This dimensional refinement, combined with advanced structural engineering of 2D membranes and 3D bulk materials, enables unprecedented thermal resistance. Significant research efforts have been devoted to creating micro/nanofiber porous thermal insulation materials, as evidenced by the consistent rise in publications over the past decade (**Figure 1a**). Multifarious raw materials, including Kevlar, nanocellulose, carbon, silk fibroin, silicon dioxide (SiO_2), and aluminum oxide (Al_2O_3), have been processed into 2D or 3D thermal insulation materials (Figure 1b).[28–37] The resulting micro/nanofiber porous materials present ultralight and excellent thermal insulation properties due to the reduced fiber diameter, elevated porosity, and hierarchical porous structure. Over the past decade, the forms of micro/nanofiber-based porous thermal insulation materials have been categorized into three types: 2D fibrous membranes, 2D aerogel fiber textile, and 3D fibrous bulk materials. Breakthrough advancements include carbon nanofiber aerogel materials developed through freeze-drying (2016), aerogel porous fibers developed through freeze-spinning (2018), and ceramic fiber sponges developed through electrospinning (2022). Recent advancements in scalability and large-scale production have greatly increased the practicality of the micro/nanofiber porous materials in the thermal insulation field. Reviews about micro/nanofiber materials application in various fields have been conducted.[10,38] For instance, Wang et al. reviewed the development of the micro/nanofiber for warmth retention, but critical examination of emergent innovations, latest progress, and strategic development pathways remains absent in current discourse.[18] Therefore, a systematic and comprehensive review is necessary to clarify the development of micro/nanofiber porous thermal insulation materials for various applications.

Herein, we provide a systematic summary of the latest advancements in micro/nanofiber-based porous materials designed for efficient thermal insulation as presented in Figure 1c. Within this framework, a detailed examination of diverse micro/nanofiber porous materials, including 2D ultrathin membranes or textiles and 3D bulks for thermal insulation, is undertaken. It focuses on methodologies for creating micro/nanofiber porous materials and explores optimization approaches to improve thermal insulation efficiency. Additionally, the representative applications of the micro/nanofiber thermal insulation materials in personal protection equipment, aerospace industry, automobile industry, and the building sector are summarized. Ultimately, the current challenges and prospects for micro/nanofiber thermal insulation materials are provided, highlighting potential research directions.

2. Thermal Transfer Theory and Performance Criteria

2.1. Thermal Transfer Mechanism

The heat flux through a material, as described by Fourier's Law, is determined by multiplying the thermal conductivity, the cross-sectional area, and the temperature gradient.[52] At the micro/nanoscale, the thermal conductivity of materials is fundamentally governed by the movement of energy carriers. Generally, thermal insulation materials with highly porous structures present low thermal conductivity (<0.1 W m^{-1} K^{-1}).[53] The heat transfer behavior of the materials could be divided into four primary components: thermal convection (λ_{conv}), thermal radiation (λ_{rad}), solid thermal conduction (λ_{sol}), and gas thermal conduction (λ_{gas}), as shown in **Figure 2a**. Understanding these mechanisms is crucial for designing advanced thermal management materials, especially for applications in harsh conditions. The total thermal conductivity (λ) of the thermal insulation materials could be estimated as:[54–56]

$$-l = -l_{conv} + l_{rad} + l_{sol} + l_{gas} \tag{1}$$

Thermal convection refers to the transfer of heat through the movement of fluids (liquids or gases) within the porous material (Figure 2b). In porous materials, thermal convection depends largely on the size of the pores and the properties of the fluid. When the pore size is sufficiently small (<1 mm), thermal convection is typically negligible.[54] This is because the fluid molecules are constrained by viscous forces, which restrict their ability to move freely. In contrast, materials with large pores could suffer from obvious convective heat transfer, particularly in the existence of temperature gradients.[57] In such cases, the fluid within the pores is able to move more freely, facilitating heat transfer. To optimize warmth retention performance, thermal insulation materials are often engineered with small and interconnected pores to suppress thermal convection.

Thermal radiation is the process of thermal energy transfer through electromagnetic waves emitted by an object with a temperature exceeding absolute 0 K (Figure 2c).[58–60] Unlike thermal conduction and convection, thermal radiation does not rely on a medium and can propagate even in a vacuum. The thermal radiative effect would obviously increase at the condition of high temperature, which can be expressed as:[61]

$$\lambda_{rad} = \frac{16 k_B n^2 T^3}{3 \rho e} \tag{2}$$

where k_B is the Stefan-Boltzmann constant, n is the average refractive index of the medium, T refers to the temperature, p signifies the density of the porous material, and e is the extinction coefficient. The equation demonstrates that the λ_{rad} scales with the third power of the temperature, suggesting that high temperatures cause a dramatic rise in thermal radiation. Additionally, the λ_{rad} is inversely related to the extinction coefficient, leading to notable differences in thermal radiation behavior among materials with varying extinction coefficients. Therefore, endowing the materials with high extinction coefficients, such as doping reflective

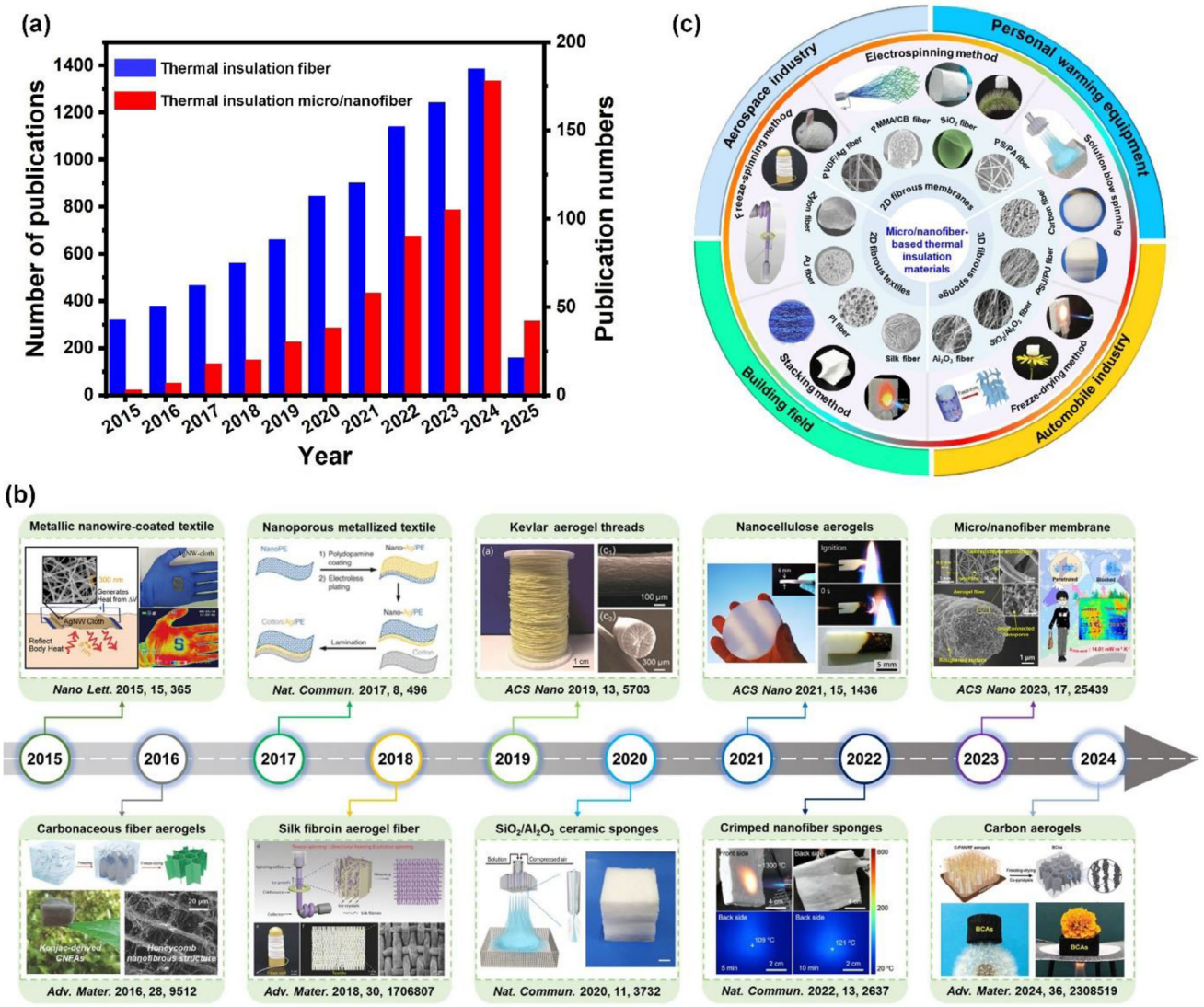

Figure 1. a) Number of publications on thermal insulation fiber and thermal insulation micro/nanofiber (data from the Web of Science). b) Summary of the advancements and innovations in micro/nanofiber thermal insulation materials. c) Micro/nanofiber-based thermal insulation materials, including 2D fibrous membranes, 2D fibrous textiles, and 3D fibrous sponges constructed by various methods. Reproduced with permission.[31] Copyright 2018, Wiley-VCH. Reproduced with permission.[33] Copyright 2020, Springer Nature. Reproduced with permission.[36] Copyright 2023, American Chemical Society. Reproduced with permission.[37] Copyright 2024, Wiley-VCH. Reproduced with permission.[39] Copyright 2023, Wiley-VCH. Reproduced with permission.[40] Copyright 2024, Springer Nature. Reproduced with permission.[41] Copyright 2024, Elsevier. Reproduced with permission.[42] Copyright 2024, Wiley-VCH. Reproduced with permission.[43] Copyright 2024, American Chemical Society. Reproduced with permission.[44] Copyright 2023, Springer Nature. Reproduced with permission.[45] Copyright 2021, American Chemical Society. Reproduced with permission.[46] Copyright 2024, Springer Nature. Reproduced with permission.[47] Copyright 2018, Association for the Advancement of Science (AAAS). Reproduced with permission.[48] Copyright 2024, American Chemical Society. Reproduced with permission.[49] Copyright 2021, American Chemical Society. Reproduced with permission.[50] Copyright 2020, Wiley-VCH. Reproduced with permission.[51] Copyright 2024, Wiley-VCH.

particles, can effectively reduce radiative heat transfer, making them suitable for high-performance insulation applications.[54,62]

Thermal conduction serves as the foundational process for heat transfer, driven predominantly by the microscale energy transport involving interacting particles (molecules, atoms), charge carriers (electrons), and quasiparticles (phonons), as shown in Figure 2d.[63] Solid thermal conduction is primarily determined by the lattice vibrations of solid molecules around fixed equilibrium points, while gas thermal conduction arises from the gas molecules. The solid thermal conduction is fundamentally governed by the inherent characteristics of materials, such as crystal structure, bonding strength, and phonon scattering. In porous materials, the solid thermal conduction is influenced by the thermal conductivity of the solid skeleton and the porosity, which can be described as:[61]

$$\lambda_{sol} = \lambda_s \frac{pv}{p_s v_s} \tag{3}$$

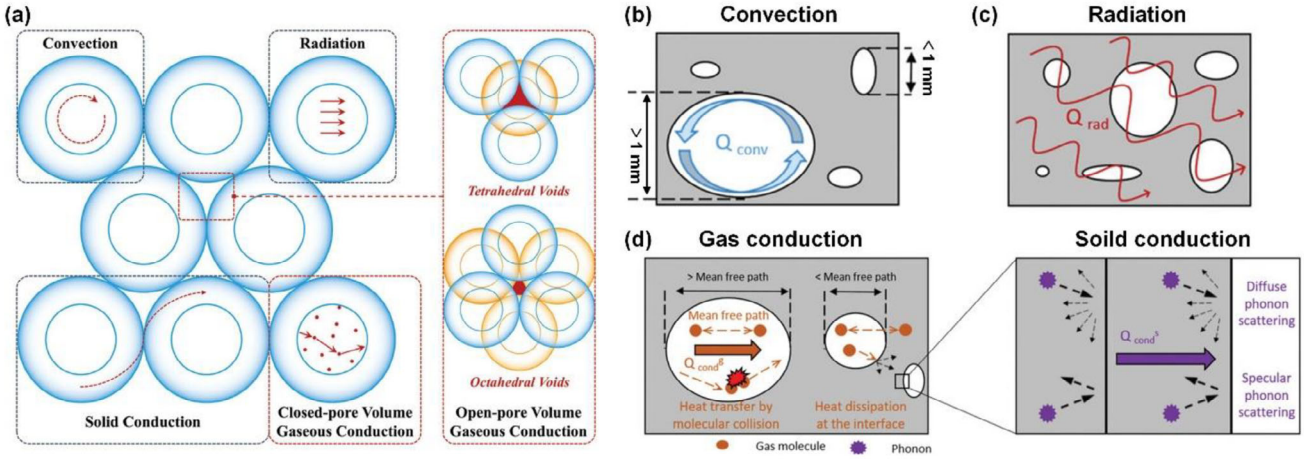

Figure 2. a) Thermal transmission pathways in porous materials. Schematic diagram of b) thermal convection, c) thermal radiation, and d) thermal conduction. Reproduced with permission.[67] Copyright 2025, Wiley-VCH. Reproduced with permission.[54] Copyright 2021, Wiley-VCH.

where λ_s is the thermal conductivity of the solid skeleton, p_s refers to the density of the skeleton, and v and v_s represent the phonon velocities in the porous material and skeleton, respectively. Concerning equation 3, enhancing the porosity of the material makes the path of heat transfer through the solid phase more tortuous, thus reducing the solid conduction effect. Additionally, introducing defects, interfaces, or nanostructures can enhance phonon scattering, further reducing solid thermal conduction.[64] Gas thermal conduction occurs through the interconnected porous channels in thermal insulation materials, which refers to the collisions between low-energy and high-energy gas molecules, resulting in heat transfer. The gas thermal conduction contribution depends on the pore size, the mean free path of gas molecules, and the specific surface area of the material. The gas thermal conduction can be expressed as:[65]

$$\lambda_{gas} = \frac{\lambda_g}{1 + \alpha K_n} \tag{4}$$

where λ_g signifies the thermal conductivity of the gas, α is the constant related to gas species, and K_n refers to the Knudsen number. The K_n serves as a dimensionless parameter to define the gas flow regime.[66] In cases where K_n is significantly greater than 1, gas molecules predominantly interact with the pore walls, with minimal collisions occurring between the molecules. On the other hand, when K_n is much smaller than 1, the gas exhibits behavior similar to a liquid, characterized by frequent intermolecular collisions. Moreover, K_n has a negative correlation with pore size, and reducing average pore sizes leads to high K_n values, which in turn decrease the effectiveness of gas thermal transfer.

In short, the thermal transfer performance of the thermal insulation materials is governed by the synergistic effects of four primary heat transfer mechanisms. Regulating the porous structure, including pore size, porosity, and tortuous channels, could effectively inhibit thermal conduction and thermal convection. Moreover, the thermal radiation could be mitigated by incorporating reflective components or nanostructures that scatter and reflect infrared radiation. By synergistically optimizing the four heat transfer paths, the thermal insulation materials could achieve exceptional thermal performance, making them highly suitable for a wide range of applications.

2.2. Evaluation Standard of Thermal Insulation Performance

The evaluation of thermal insulation performance in fibrous porous materials, namely interconnected fiber networks with substantial void spaces, is critical for determining their suitability in various applications. To ensure consistency and reliability, standardized testing methods have been established, including steady-state methods and transient methods.[68,69] Steady-state methods are employed to assess thermal conductivity under conditions where the temperature differential across a material stays constant throughout time. The methods are highly accurate and widely used for low-medium thermal conductivity materials. Two typical measurement equipment of steady-state techniques are the guarded hot plate and flow meter apparatus. The guarded hot plate involves placing a sample between two plates: a hot plate that is maintained at a constant high temperature and a cold plate that is kept at a stable low temperature.[54,70] By measuring the temperature difference across the sample and the heat flux, the material's heat transfer capability can be quantitatively determined using Fourier's law of heat conduction. This equipment is suitable for homogeneous materials with low thermal conductivity, such as fiber mats. The principle of the flow meter apparatus is that the heat flow sensor measures the heat flux through the specimens and the temperature sensors monitor the temperature difference across the sample.[71] By analyzing the heat absorbed by the fluid, the flow rate, and the temperature gradient, the material's thermal conductivity can be determined. This method is particularly ideal for materials with moderate thermal conductivity, such as fiber-based composites.

Compared with the steady-state techniques, the transient techniques measure samples under non-steady-state conditions, which are frequently employed to evaluate the thermal conductivity of small samples quickly.[54,72] The transient techniques mainly refer to the transient plane source and laser flash method. The transient plane source uses the flat sensor, acting as both a

heat source and a temperature sensor, to record over time the heat transfer through the sample. By analyzing the temperature rise and the rate of heat diffusion, the material's thermal conductivity and thermal diffusivity can be measured simultaneously. The method is highly versatile, fast, and suitable for a wide range of materials, including 2D membranes or 3D bulk materials. The laser flash method is a non-contact, non-invasive, and transient approach used to determine thermal diffusivity.[73] In this method, a circular sample is exposed to a short pulse of laser energy on one side, which rapidly heats the surface. The thermal diffusivity of the materials can be obtained by analyzing the time-dependent temperature response. The laser flash technique offers exceptional measurement precision while maintaining sample integrity, making it applicable to diverse material systems from conductive alloys to engineered ceramics and multiphase composites. Despite many advantages, the transient techniques still have certain limitations. First, measurement accuracy may be compromised for highly porous or anisotropic materials due to insufficient heat penetration or inhomogeneous heat distribution. Moreover, transient methods often assume ideal boundary conditions, which may not hold for ultra-lightweight fibrous materials with high interfacial thermal resistance. Furthermore, some special thermal insulation materials, such as resin-based fiber insulation materials, would undergo pyrolysis under high-temperature conditions, thus presenting significant challenges in testing thermophysical properties. The thermophysical properties of resin-based fibrous materials during pyrolysis can be characterized through a combination of experimental and computational methods. Key techniques include thermogravimetric analysis for pyrolysis kinetics, transient hot-wire methods for thermal conductivity, and laser flash analysis for thermal diffusivity. Additionally, multiphysics modeling, such as finite element analysis coupled with reaction kinetics, could be adopted to address the coupled heat and mass transfer challenges.

3. 2D Micro/Nanofibrous Membranes and Textiles

2D thermal insulation materials, providing exceptional warmth retention while maintaining lightweight and compact characteristics, have been widely concerned by academia and industry. Especially, the ultrathin characteristic of the 2D materials could save space and provide flexibility in design, allowing for easy integration into various applications. In recent years, a variety of ultrathin thermal insulation materials have been reported, which mainly include two principal categories, referring to the thermally insulating micro/nanofibrous membranes and aerogel fiber textiles. In this section, the structural regulation and thermal insulation performance optimization of the two materials mentioned above are summarized and discussed.

3.1. Micro/Nanofibrous Thermal Insulation Membranes

Fiber materials have long been regarded as appealing options among the various warmth retention materials because of their high degree of comfort, accessibility, and low cost.[74,75] However, these fibrous flocculus materials, such as cotton, polyester, and wool, suffer from moderate thermal insulation performance due to their relatively large pore size and limited porosity.[45] Compared with the traditional fibers, the advanced micro/nanofibers with small aperture and enhanced porosity could efficiently capture still air to limit heat conduction, demonstrating great promise in efficient thermal management applications.[36] In the last decade, there have been rising ways to fabricate micro/nanofibrous thermal insulation membranes, which could fall into two types based on their chemical composition and functional characteristics: polymer-based fibrous membranes and inorganic fibrous membranes. A detailed description of the fabrication methods, structural characteristics, and properties of the two types is provided below.

3.1.1. Polymer-Based Fibrous Membranes

Polymer-based fiber materials, featuring an attractive combination of low density, ultrathin thickness, low thermal conductivity, and flexible surface, have great application prospects in the field of thermal insulation.[76–78] Up to now, many strategies have been used to construct high-performance thermal insulation fibrous membranes, among which the most common methods are to improve the infrared reflection ability and to reduce the thermal conduction of the fibrous membranes. It is reported that about 40–60% of the heat loss in the human body is caused by thermal radiation.[79] To reduce the radiative heat dissipation, Hsu et al. first attempted to coat the silver nanowires (AgNWs) onto normal cotton fabrics.[28] Benefiting from the reflecting human body infrared radiation, low emissivity, and satisfactory plasma properties of metallic nanowires network, the designed AgNW-cloth not only possesses excellent thermal insulating properties but enables passive insulation via Joule heating. In contrast to the conventional cotton cloth (1.3%), the AgNW-cloth achieved a high human body radiation of 40.8%. More importantly, the AgNW-cloth could quickly heat up to 38 °C after applying the 0.9 V voltage, higher than the average human body temperature (37 °C). These promising results exemplify the validity of the method by coating the metal nanowires on the surface of fibrous substrates to develop high-efficiency warmth retention materials.

Inspired by the AgNW-cloth, various polymer-based membranes with active warmth retention have been created by combining the metal nanowires with the micro/nanofibers. For example, Gao et al. fabricated the flexible dual-sided polyimide (PI) nonwoven with tailored breathability and thermal properties by coating AgNWs into the surface of PI nanofibrous membranes.[80] Compared with the normal textiles, the developed composite membranes exhibited excellent infrared (IR) reflectance of more than 80% and low electrical resistance of 0.23 Ω sq^{-1}. Significantly, the membranes could raise the surface temperature to 37 °C by applying a low current of 0.2 A, which is similar to the temperature of human skin, demonstrating potential application in personal thermal management devices. Coating metal nanowires, such as AgNWs and CuNWs, on the surface of the micro/nanofibrous membranes could indeed improve the thermal insulation performance. However, the Ag materials are easily oxidized when exposed to air and peeled off the fibrous membrane substrate, resulting in limited application in the energy-saving field.[81] To solve the bottleneck problem, an effective strategy of doping AgNWs in 1D nanofibers was proposed

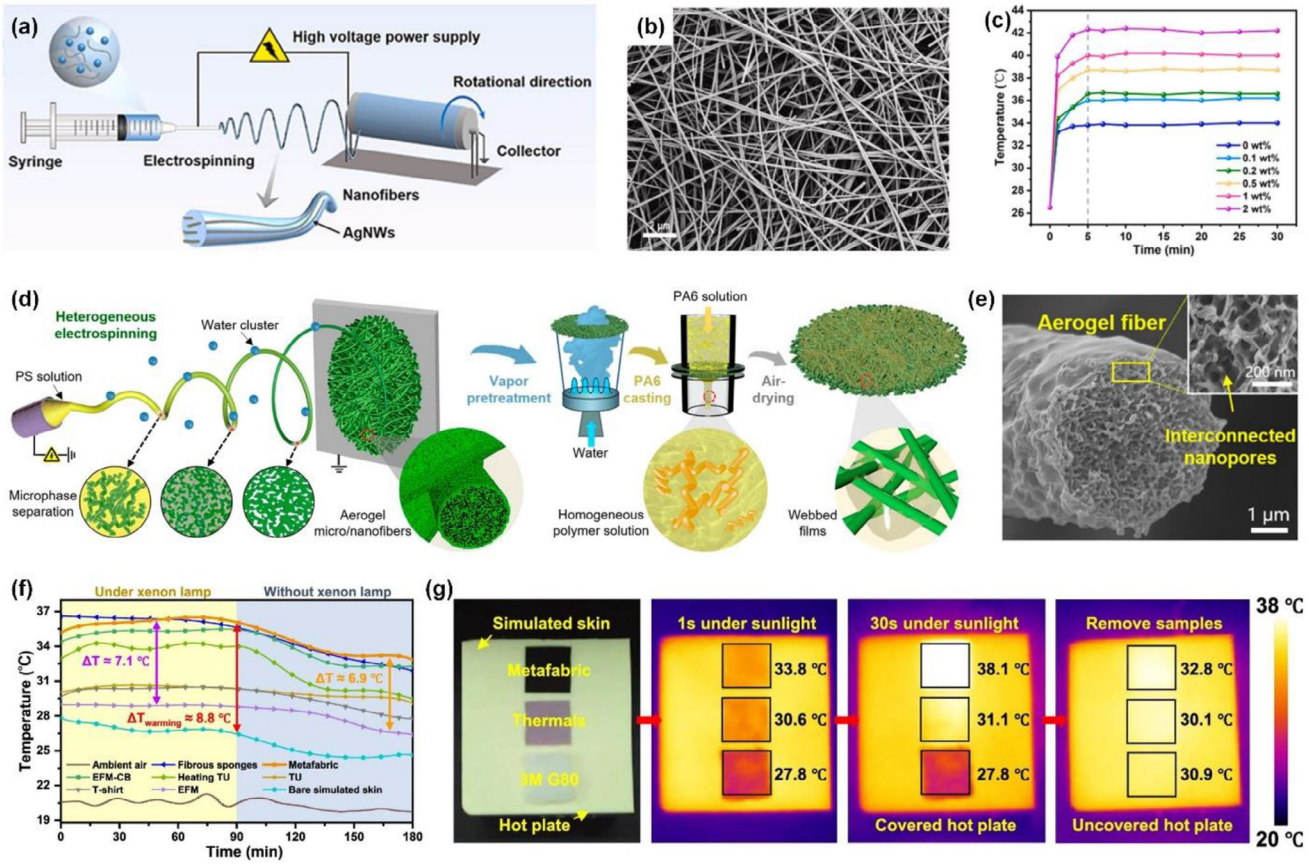

Figure 3. a) Schematic illustration of fabricating the PVDF/AgNWs nanofibrous membrane. b) TEM image of PVDF/AgNWs nanofibers. c) Surface temperature of the membranes under the irradiation of 100 mW cm^{-2} light intensity. d) The fabrication of the hierarchical cellular-structured porous micro/nanofiber membranes. e) Microstructure of the membranes. f) Temperature variation curve of skin simulators covered by different fabrics. g) Comparing the thermal insulation performance of different fabrics. Reproduced with permission.[41] Copyright 2024, Elsevier. Reproduced with permission.[36] Copyright 2023, American Chemical Society. Reproduced with permission.[40] Copyright 2024, Springer Nature.

to protect the AgNWs from contamination, corrosion, and oxidation. A representative example was given by incorporating AgNWs into polyvinylidene fluoride (PVDF) precursor solutions to form nanofibrous membranes via electrospinning technology (**Figure** 3a).[41] Originating from the shearing effect of the solution and the drawing impact of the high-voltage electrostatic field, the AgNWs were wrapped in PVDF fibers and aligned along the fiber direction (Figure 3b). Ultimately, the developed PVDF/AgNWs nanofibrous membranes showed good air permeability of 75 mm^{-1} and low thermal conductivity (18 mW m^{-1} K^{-1}). Interestingly, derived from the in situ doping of AgNWs, the surface temperature of the membranes could reach ≈43 °C after 5 min of irradiation and can almost maintain a constant temperature, demonstrating stable and long-lasting thermal insulation performance (Figure 3c).

Another facile strategy to develop high-performance thermal insulation membranes is to construct porous structures on micro/nanofibers. The thermal insulation mechanism of porous fibers is that they contain a large number of tiny pores, which can trap air molecules, thereby preventing heat transfer.[82] The thermal conductivity of porous materials can be adjusted by optimizing the porosity, pore size, and pore structure. Especially, when the size of the pores in the fiber is smaller than the free path of the gas molecule (≈66 nm), the nanoscale pores can block the flow of air molecules and heat conduction according to the Knudsen effect, providing remarkable warmth retention. A good example was provided by creating porous micro/nanofiber membranes with a hierarchical porous structure via combining the electrospinning and solution casting methods (Figure 3d).[36] The microphase separation of the charged jets during electrospinning was manipulated by regulating the polymer concentration and spinning humidity to form the nanopores inside the fibers (Figure 3e). Subsequently, cellular structures between fibers were constructed by tailoring the phase separation of the spreading casting solution. Ultimately, the obtained hierarchical cellular structured micro/nanofiber membranes exhibited high porosity, ultrafine fiber diameter, and ultrathin thickness (≈0.5 mm). Meanwhile, derived from the porous structure and tiny nanopores (≈30–60 nm), the ultrathin micro/nanofiber membranes possessed ultralow thermal conductivity (14.01 mW m^{-1} k^{-1}), demonstrating superior warmth retention performance. Although constructing hierarchical microporous structures can reduce thermal conductivity, the single mode of controlling heat conduction has limited improvement in thermal

management. Incorporating passive and active thermal structures may efficiently solve the problems. Inspired by the microstructure of sunflower achieved enhanced light harvesting and energy retention capabilities, Tian et al. developed ultrathin micro/nanofiber metafabric via in situ introducing size-matching carbon black (CB) nanoparticles into the nanopores of polymethyl methacrylate (PMMA) nanofibers.[40] The generation of the porous PMMA nanofibers relies on water diffusion, molecular chain movement, and phase separation within electrospun jets. As water diffuses into the jet, the fluorocarbon chains facilitate polymer molecule aggregation, inducing microphase separation in the solution to form the pores. Combining the multi-scattering of the nanoparticles and the Knudsen effect of nanopores facilitated thermal energy storage in the metafabric. As a result, the developed membranes present low thermal conductivity (15.8 mW m^{-1} K^{-1}) and satisfactory heat storage performance with 65% radiant energy retention. Meaningfully, the temperatures of the metafabrics were 5.6, 5.8, 7.2, and 9.3 °C higher than the commercial TU membranes, T-shirt, electrospun fibrous membranes, and bare skin simulators, respectively, under a Xenon lamp within 90 min (Figure 3f). Moreover, the temperature of the simulated skin covered by the metafabrics was 2 °C warmer than the 3M fibrous sponge, further confirming superior thermal regulation capabilities (Figure 3g).

In addition to the strategies mentioned above, doping the phase change materials or humidity-stimulated self-heating materials into the fibers has also been developed to improve thermal insulation materials. For example, Chen et al. reported that humidity stimulated adaptive heating materials by utilizing the aluminum core-liquid metal shell microparticles as fillers.[83] The materials could react with surrounding water molecules to generate heat, thus providing thermal protection in extreme conditions. Although a series of polymer-based thermal insulation membranes have been developed, several challenges still remain. One major issue is the difficulty in achieving both high thermal resistance and mechanical strength simultaneously, as reducing thickness often compromises durability. Additionally, maintaining consistent performance under extreme temperatures or harsh environmental conditions remains a significant hurdle. Addressing these issues is crucial to improving the application performance of thermal insulation fibrous membranes.

3.1.2. Inorganic Fibrous Membranes

Inorganic fibrous membranes possess unique properties of high-temperature resistance, good chemical stability, and lightweight, making them widely used in harsh thermal protection fields.[84–86] At present, commercial inorganic fibrous membranes mainly include SiO_2 fiber, Al_2O_3 fiber, mullite fiber, aluminum silicate fiber, and so on. The problem with the common inorganic fiber is the large fiber diameters (usually >5 µm), resulting in high thermal conductivity. It is widely recognized that reducing fiber diameter, especially refined to the order of nanometers, would increase the heat transfer path and improve the thermal insulation performance. Recently, various methods, including sol-gel, template synthesis, and electrospinning, have been reported to fabricate inorganic nanofiber membranes. Among these techniques, electrospinning is thought to be a promising strategy for manufacturing inorganic nanofibers, attributed to a wide source of raw materials, relative simplicity, and ease of scalability. At present, the electrospun inorganic nanofibers for high-temperature insulation mainly involve SiO_2, zirconium oxide (ZrO_2), Al_2O_3, and so on.[87] Those materials have been widely investigated for their remarkable thermal insulation performance and appropriateness for a range of industrial applications needing high-temperature conditions.

In 2002, Shao et al. first reported the SiO_2 nanofibers by using polyvinyl alcohol (PVA) as a template and tetraethoxysilane sol as a silicon source based on sol-gel electrospinning.[88] The fabricating process of the SiO_2 nanofibers involved the preparation of PVA/SiO_2 precursor solutions, electrospinning, and calcination. This study also investigated the effect of calcination temperature on the morphology and crystallization behavior of SiO_2 nanofibers. The results illustrated that the amorphous SiO_2 nanofibers with diameters of 200–400 nm were obtained. To enhance the mechanical property, Si and co-workers prepared the ultra-softness and improved tensile strength of SiO_2 nanofibrous membranes via doping NaCl into the sol-gel solution to generate a bonding structure between SiO_2 nanofibers.[89] Besides, the morphology and mechanical properties of the materials were systematically optimized by regulating the NaCl content and the calcination temperature. The developed SiO_2 nanofibrous membranes showed a robust tensile strength of 5.5 MPa, ultra-softness of 40 mN, and ultra-low thermal conductivity (0.0058 W m^{-1} K^{-1}). Such soft inorganic nanofibrous membranes are expected as promising candidates for bunker clothing. Similarly, to improve the tensile strength, Liu et al. proposed the self-templated electrospinning strategy to fabricate the SiO_2 nanofibers without adding a polymer template.[39] The core of this method is to control the ratio of water to TEOS to be ≈2, thereby forming a spinnable linear silica molecular chain. The resulting nanofibers have dense and defect-free structures, exhibiting a satisfactory tensile strength of 1.41 GPa. Despite currently developed SiO_2 nanofibers possessing high toughness and strength, there is a lot of potential to enhance the mechanical and heat insulation capability of inorganic nanofibrous membranes because of the absence of a stable interfacial connection between nanofibers.[90] Therefore, Mao and co-workers developed a facile reinforcement method for constructing mechanically stable inorganic nanofibrous membranes with extraordinary temperature resistance via cross-linking the ZrO_2-SiO_2 nanofibers and montmorillonite (MMT) nanosheets (**Figure 4a**).[91] The methodological systems refer to fabricating precursor solution of polyvinyl pyrrolidone (PVP), zirconium acetate, and TEOS, generating ZrO_2-SiO_2 nanofibers based on one-step electrospinning and calcination, and cross-linking assembled with MMT nanosheets. The ultrathin MMT nanosheets, similar to solid walls, are bonded in the ZrO_2-SiO_2 fiber matrix (Figure 4b). Benefiting from the interfacial interaction between the nanofibers and the nanosheets, the resulting membranes exhibited a low thermal conductivity of 0.026 W m^{-1} K^{-1} and temperature-invariant mechanical stability from −196 to 1000 °C. The surface temperature of the inorganic membranes was ≈39.6 °C after being heated by the heating plate for 2 min, highlighting the exceptional heat insulation capability (Figure 4c).

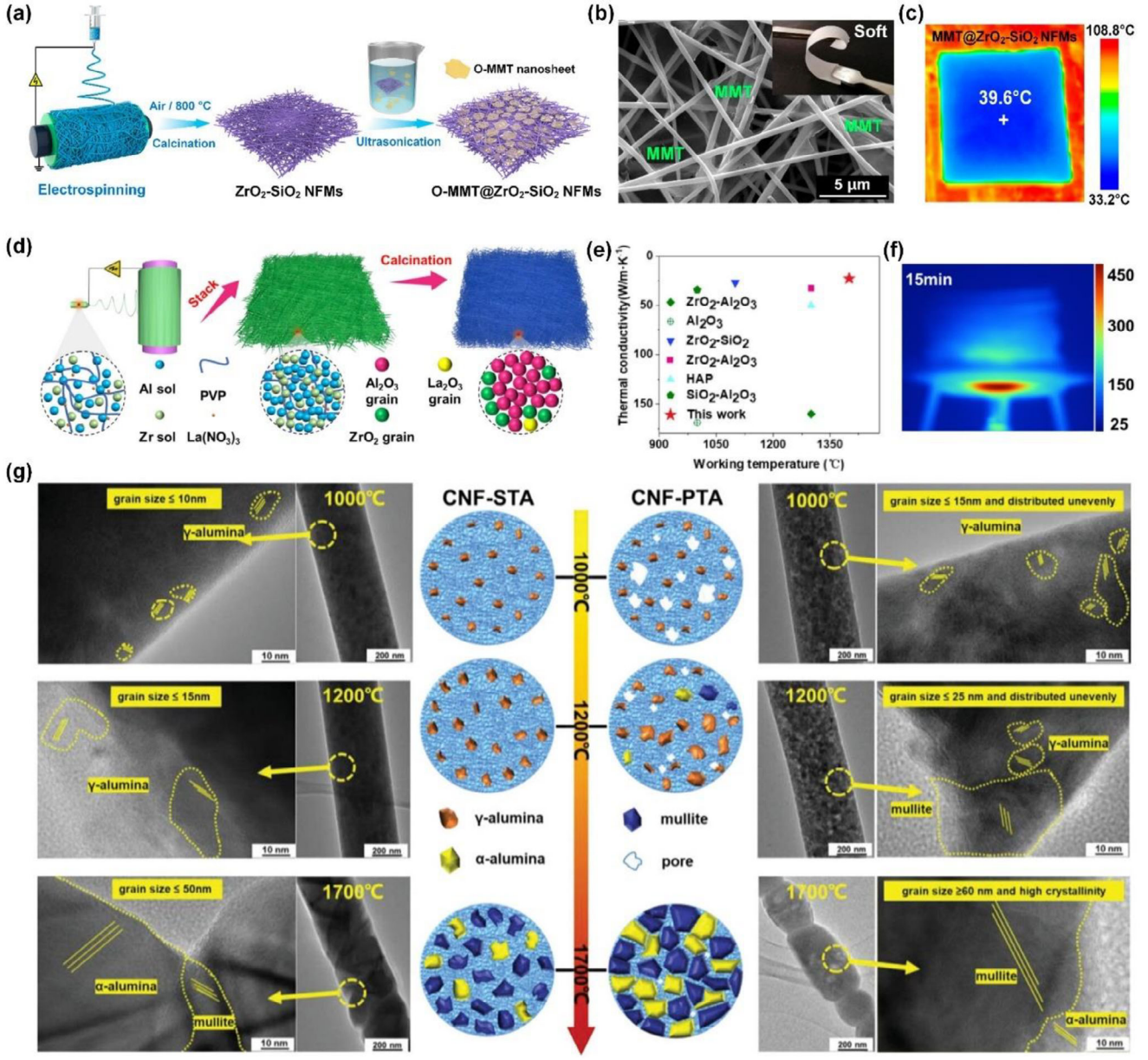

Figure 4. a) Schematic diagram of the preparation for MMT@SiO_2-ZrO_2 NFMS. b) SEM image of the membranes. c) Demonstration of thermal insulation property of the membranes. d) Presentation of the synthetic steps of AZLNMs. e) Comparing the working temperature and thermal conductivity. f) The infrared camera photos of the membranes on the burning ethanol flame. g) The difference between microstructures of self-templated nanofibers and polymer-templated nanofibers calcined at typical temperatures. Reproduced with permission.[91] Copyright 2021, American Chemical Society. Reproduced with permission.[93] Copyright 2023, Elsevier. Reproduced with permission.[95] Copyright 2023, Wiley-VCH.

Compared with SiO_2 fibers, Al_2O_3 fibers can withstand higher temperatures and be applied in more harsh environments, thereby garnering widespread research interest.[38] Wang et al. using aluminum isopropoxide as the precursor, prepared the Al_2O_3 nanofibers via electrospinning and calcination treatment.[92] As a result, the membranes could bear heat treatment at 1200 °C and showed a low thermal conductivity of 0.318 $W\,m^{-1}\,K^{-1}$ at 1000 °C. To enhance the elastic performance and compression resistance of inorganic nanofibers, Li and co-workers prepared multi-phase ceramic nanofibers consisting of Al_2O_3, ZrO_2, and La_2O_3 via sol-gel electrospinning (Figure 4d).[93] The La_2O_3 and ZrO_2 gather at the grain boundary of Al_2O_3 nanograins, thus forming the small grain. Compared with reported ceramic materials, the $Al_2O_3/ZrO_2/La_2O_3$ nanofibrous membranes (AZLNMs) presented exceptional insulating performance with thermal conductivity of 22.67 $mW\ m^{-1}\ K^{-1}$ (Figure 4e). Moreover, the membranes can maintain outstanding elasticity and compressibility at the temperature of 1400 °C. More importantly, the AZLNMs could continuously tolerate a high-temperature ethanol flame,

demonstrating high-temperature thermal stability (Figure 4f). Such high-temperature resistant ceramics show a wide application prospect in firefighting protective clothes, new energy, and electronic products. Nevertheless, for extremely high-temperature environments (>1500 °C), the common inorganic ceramic fibers would be rapidly destroyed due to the irreversible growth of grains, failing to meet the application requirements.[94] Therefore, Xu et al. proposed an original template-free spinning strategy to create alumina-based nanofibers with exceptional strength even at harsh temperatures (Figure 4g).[95] On the one hand, the inorganic molecular chains were successfully synthesized by modifying the metal alcohol salt, which showed a similar spinnability to the polymer. On the other hand, the massive silicon components were introduced into aluminum-based fiber to restrain grain growth at high temperatures. As a result, the obtained ceramic nanofibers possessed impressive flexibility and high tensile strength of 1.02 GPa even being exposed to 1700 °C. Such high strength achieved on ceramic fibers at 1700 °C is barely reported.

In addition to the conventional thermal insulation fibers, researchers have engineered novel inorganic types to boost mechanical strength and heat retention capabilities, such as TiO_2 fiber, Y_2O_3 fiber, MgO fiber, $Y_2Zr_2O_7$ fiber, and mullite nanofiber.[38,87] For example, Guo et al. fabricated mullite nanofiber membranes via electrospinning, employing polyethylene oxide and PVA as dual templates.[96] Polymer templates are essential for regulating the viscosity of mullite electrospinning solutions and significantly affect their spinnability. The obtained membranes exhibited superior high-temperature resistance (>1300 °C) and exceptional thermal insulation with low thermal conductivity (0.035 W m^{-1} K^{-1}). Although various kinds of inorganic thermal insulation fiber materials with low thermal conductivity have been developed, challenges remain in optimizing the balance between thermal insulation, flexibility, and durability, as well as in scaling up production for commercial applications. Future research should focus on exploring novel material compositions, refining fabrication methods, and investigating the long-term performance of these materials under real-world conditions to realize their potential in industries ranging from aerospace to new energy.

3.2. Aerogel Fiber Textile

Thermal insulation materials based on fibrous membranes have long been recognized for their inherent properties of ultra-thinness, flexibility, and tunable porosity. However, the pursuit of higher performance and multifunctionality in thermal insulation has driven the development of advanced materials, among which aerogel fiber-based textiles stand out as a revolutionary innovation. Unlike conventional fibrous membranes, aerogel fibers, deriving from aerogels with the 3D network, abundant porosity, small pore size, and large surface area, offer superior insulation performance while maintaining lightweight and flexible characteristics. Recent advancements in fabrication techniques, such as freeze spinning and wet spinning technology, have further enhanced the scalability of aerogel fibers, paving the way for their integration into next-generation thermal insulation solutions. The following sections explore the unique properties, fabrication methods, and emerging applications of aerogel fiber-based textiles, underscoring their potential in thermal insulation materials.

3.2.1. PI-Based Aerogel Fiber Textile

PI stands out as a high-performance polymer due to its exceptional combination of thermal stability (>400 °C), mechanical strength, and chemical resistance, making it ideal for extreme environments.[97,98] Therefore, PI-based aerogel fibers have gained widespread attention. Mimicking the hierarchical pore organization of polar bear hair, Wang et al. first developed the porous PI aerogel fiber for thermal insulation textiles based on the freeze-spinning method.[99] As shown in **Figure 5a**, the detailed fabrication process of PI aerogel fiber included the fabrication of water-soluble poly(amic acid) precursor, freeze spinning, freeze drying, and thermal imidization. From the cross-sectional SEM image, the well-aligned pores in the PI fiber could be observed (Figure 5b). Such a highly porous structure is conducive to the storage of large amounts of still air, providing efficient warmth retention. Although the developed PI aerogel fiber with high porosity has a broad application prospect in the field of thermal insulation, some key problems still exist. First, compared with the inorganic silica aerogels, the PI aerogel fiber textiles still present higher thermal conductivity. Second, to obtain the porous structure of aerogel fibers, the supercritical-drying or freeze-drying treatment is employed, which is time and cost-consuming. Third, the PI aerogel fiber shows poor mechanical performance due to the highly porous structure, limiting its practical application. Therefore, a lot of research has been done to solve the above problem.

To further improve the thermal insulation performance, Xue and co-workers engineered ultralight PI aerogel fibers with exceptional thermal insulation properties through a freeze-spinning technique, utilizing PVA as a pore-regulating agent.[100] The strong interaction between PVA and water facilitates the rapid nucleation of ice crystals, modulates pore formation, and establishes a well-defined porous architecture in the PI aerogel fibers. As a result, the obtained PI aerogel textiles showed excellent thermal insulation with a low thermal conductivity of 28.7 mW m^{-1} k^{-1} and could work under high temperatures (up to 300 °C). Incorporating inorganic porous nanomaterials into PI aerogel fiber is also an effective method to enhance their thermal insulating performance. A typical example is the development of double-network organic/inorganic PI/SiO_2 aerogel fiber via co-gelation and freeze-spinning technique.[101] Benefiting from the cooperative reinforcement between the SiO_2 network and PI frameworks, the obtained PI/SiO_2 aerogel fiber fabrics demonstrated low thermal conductivity in harsh environments (75.6 mW m^{-1} k^{-1} at 350 °C) and excellent thermal stability. More importantly, the aerogel fabrics effectively inhibit thermal transfer in high-humidity conditions, exhibiting a thermal conductivity of 58.8 mW m^{-1} K^{-1} at 80 °C and 100% relative humidity, owing to their strong hydrophobicity.

To solve the time-consuming and scalable production, Xue et al. proposed a novel approach combining wet-spinning and ambient pressure drying by UV-enhanced dynamic gelation (Figure 5c).[44] This approach facilitates a rapid sol-gel

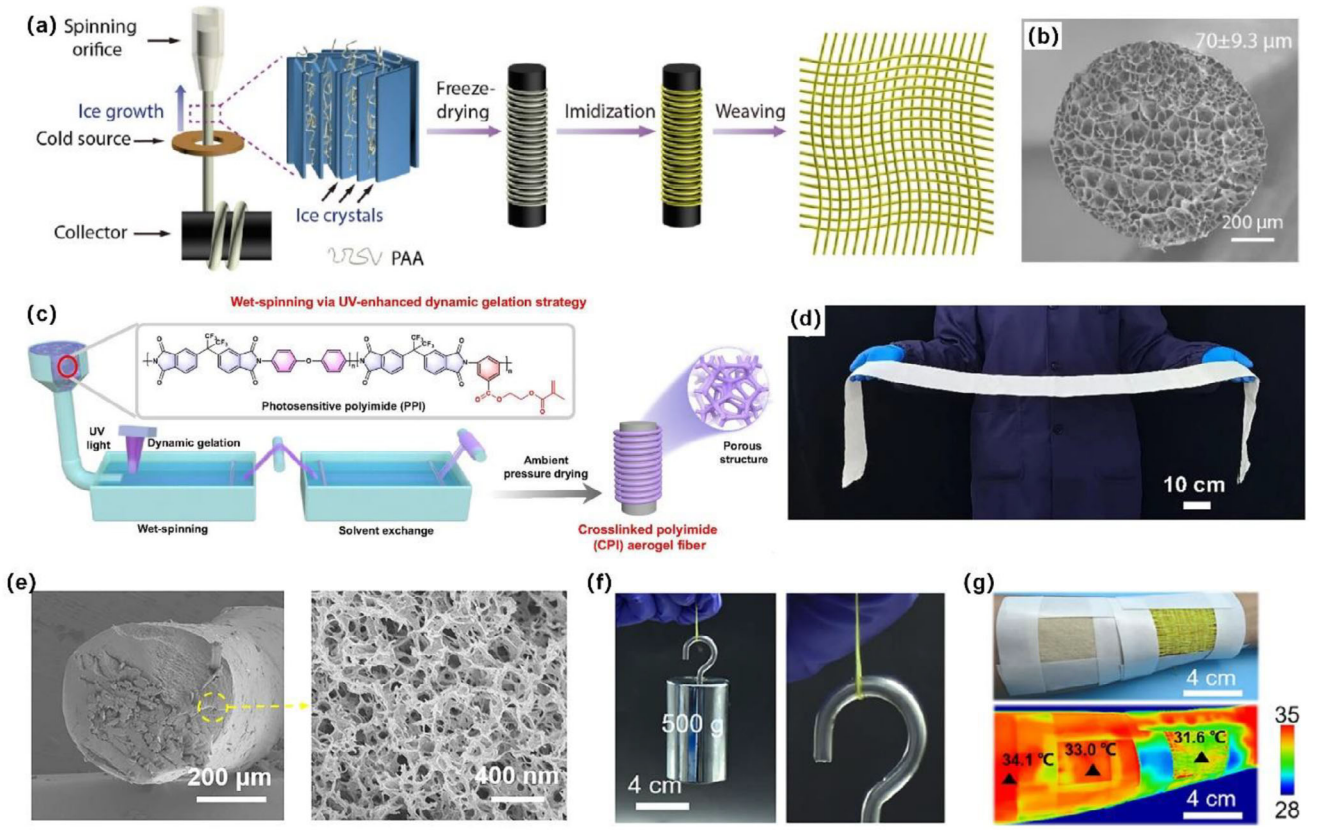

Figure 5. a) The fabrication process of PI aerogel fiber and textiles. b) The cross-sectional image of the fiber. c) Schematic illustration of preparing aerogel fibers. d) Photograph of the large-sized aerogel fiber textile. e) Cross-sectional SEM image of LPF-PAF aerogel fiber illustrating the porous structure. f) The mechanical properties display of single aerogel fiber. g) Comparing the thermal insulation performance. Reproduced with permission.[99] Copyright 2020, Elsevier. Reproduced with permission.[44] Copyright 2023, Springer Nature. Reproduced with permission.[102] Copyright 2023, American Chemical Society.

transformation in photosensitive PI, creating a densely crosslinked gel framework that preserves the fiber morphology and nanoporous architecture. A continuous manufacturing protocol achieved meter-scale (>100 m) PI aerogel fiber outputs within 7 h of processing time, significantly more efficient than earlier techniques (>48 h). The large-size PI aerogel fiber fabrics with lengths larger than 1 m could be woven by a semi-automatic weaving machine, as illustrated in Figure 5d. The resulting ultrathin aerogel fabric, with 0.7 mm thickness (≈1/8 that of down), demonstrates the same thermal insulation performance as down. This study opens significant opportunities for the large-scale and economical production of advanced multifunctional aerogel fibers, showcasing the immense potential for applications in personal thermal management.

To enhance the mechanical properties, Zhu et al. prepared the durable and thermally insulating long PI fiber-reinforced PI aerogel fiber (LPF-PAF).[102] Utilizing an injection technique combined with a rubber tube-assisted molding process, the LPF-PAFs with a core-sheath structure were fabricated. The sheath, composed of porous crosslinked polyimide aerogel, imparts excellent thermal insulation properties, while the core, made of long polyimide fibers, ensures exceptional mechanical strength (Figure 5e). Interestingly, the single LPF-PAF is capable of supporting a 500 g weight without fracture, highlighting its remarkable mechanical strength (Figure 5f). Additionally, the fabric woven from LPF-PAFs, as shown in Figure 5g, demonstrates significantly enhanced thermal insulation performance over conventional cotton textiles, indicating its promise for protective apparel applications. In the textile industry, single yarn is often processed into twisted strands to enhance its mechanical properties. Inspired by the design concept, Tafreshi et al. reported the fabrication of aerogel fiber bundles with twisted structures via combining the sol-gel confined transition method and fiber twisting technique.[103] A comprehensive investigation was conducted to evaluate the influence of design parameters on the mechanical properties of the fiber bundles. Eventually, the tested aerogel fibers exhibited an elastic modulus of ≈7.6 MPa, alongside an ultimate stress of about 1.25 MPa, and an ultimate strain of 29%. The creation of aerogel fiber bundles with twisted structures paves the way for the development of mechanically robust thermal retention textiles.

3.2.2. Other Aerogel Fiber Textile

In addition to the PI polymer discussed above, silk fibroin, chitosan, Zylon, PU, etc., were also employed to develop aerogel

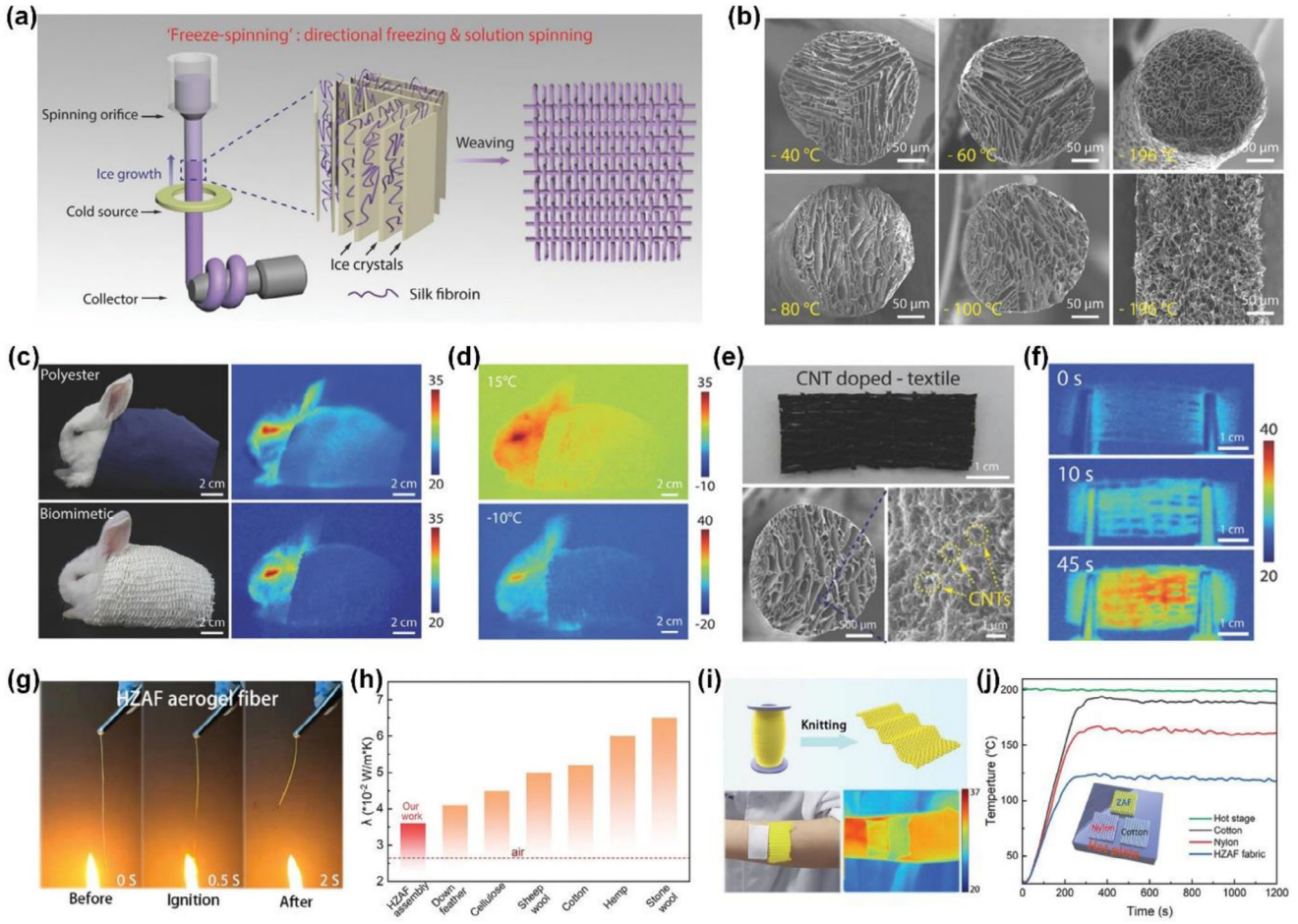

Figure 6. a) Presentation of fabricating the aerogel fiber with an aligned porous structure based on the freeze spinning method. b) Cross-sectional images of aerogel fiber obtained from various freezing temperatures. c) Optical and IR image of the rabbit covered by polyester textile and aerogel fiber textile. d) Demonstrating the thermal illustration of aerogel fiber textile. e) Microstructure of the aerogel fiber doped with CNTs. f) IR images of the CNT-doped aerogel fiber textile after applying voltages. g) Ignition test of HZAFs. h) Comparing the thermal conductivity of different thermal insulation materials. i) Optical and IR images illustrating the thermal insulation performance of the aerogel fiber textiles. j) Temperature changes versus time of HZAFs fabrics, cotton, and Nylon insulation materials placed on the hot table. Reproduced with permission.[31] Copyright 2018, Wiley-VCH. Reproduced with permission.[42] Copyright 2024, Wiley-VCH.

fiber textiles for thermal insulation applications. For example, Cui and co-workers, mimicking polar bear hairs, prepared the silk aerogel fiber with an aligned porous structure via the freeze-spinning method.[31] As depicted in **Figure 6a** , the manufacturing process of silk aerogel fiber includes the fabrication of silk fibroin solution, freeze spinning, and freeze drying. Exhibiting comparable phase-separation behavior to conventional freeze-casting, the freeze-spinning technique leverages ice crystal kinetics to engineer tailored pore morphologies. Figure 6b demonstrates the successful fabrication of aerogel fibers with an aligned porous structure, which could be regulated by changing the freezing temperature. Such a highly porous structure could store a lot of still air, reducing the heat transfer. Moreover, aligned pores are deemed more conducive to reflectance compared to random pores, due to a "multiple reflective effect" with a consistent incident angle. Significantly, the infrared images of a rabbit wearing the aerogel fiber fabric maintained a surface temperature closer to the ambient environment, highlighting its exceptional thermal resistance relative to the same-thickness polyester fabrics (Figure 6c,d). To ensure effective personal thermal management, materials must incorporate not only passive insulation but also active heating capabilities. Doping conductive materials, such as carbon nanotubes (CNTs), AgNWs, and CuNWs, into the aerogel fibers is an effective strategy to improve thermal insulation properties. A typical example is the fabrication of silk/CNTs aerogel fiber via the freeze-drying method with CNTs dispersed into the silk fibroin solution. As shown in Figure 6e, the CNTs are uniformly dispersed and integrated into the aerogel fiber while preserving the aligned porous microstructure. Meaningfully, upon integrating the textile into an electrical circuit and applying a voltage of 5 V, the surface temperature rises swiftly from ≈24 to 36.1 °C in just 45 s, demonstrating the excellent active thermal management capability (Figure 6f). Although the developed aerogel fiber fabric exhibits superior thermal insulation performance, the application of aerogel fibers in textiles has been significantly restricted due to their inherent

brittleness and limited processability, often leading to irreversible structural damage and a consequent decline in thermal insulation efficiency during practical application. To solve the bottleneck, Wu et al. proposed a facile strategy by mimicking the core-shell structure of polar bear hair and encapsulating the aerogel fiber with an elastic thermoplastic polyurethane (TPU) layer.[104] The aerogel fibers were first prepared by the freeze-spinning and freeze-drying techniques, and then the fibers were encapsulated through solution-phase TPU deposition and subsequent controlled drying. The encapsulating outer layer not only enhances the mechanical strength of the aerogel fiber but also protects its thermal insulation capabilities during repeated stretching cycles. Astonishingly, the aerogel fibers were washable and dyeable, and could retain the thermal retention performance after 10 000 stretching cycles (100% strain). Moreover, a sweater made from the fiber achieved comparable performance to down while being just one-fifth the thickness. Such aerogel fiber textiles offer exceptional thermal insulation and versatility, making them highly suitable for applications in extreme cold conditions.

Considering the solvent corrosion and high-temperature environment faced in the practical application, Hu et al. proposed a novel approach to prepare hierarchical Zylon aerogel fibers (HZAFs) through synergistic proton-regulated gelation spinning and thermal crosslinking.[42] The innovative synthetic pathway for preparing the HZAFs includes the fabrication of Zylon sol fibers, sol-gel transition based on the coagulation bath, solvent exchange, and supercritical drying. Eventually, the HZAFs revealed robust thermal stability and extreme chemical resistance. As shown in Figure 6g, when exposed the HZAFs to flame, thermal shrinkage and carbonization decomposition take place, but the flame fails to spread owing to the high thermal decomposition temperature and carbon content, demonstrating the high flame retardancy. Benefiting from the high porosity (98.6%), the HZAFs exhibited low thermal conductivity (0.036 W m^{-1} K^{-1}), significantly lower than the reported down feather, cotton, and wool (Figure 6h). Moreover, the HZAF textile covering the skin exhibited a lower surface temperature compared to the cotton fabric, highlighting the excellent thermal insulation capabilities (Figure 6i). To further assess the thermal insulation properties in a high-temperature environment, the textiles were heated by heating resource (200 °C) to observe the change in surface temperature, as shown in Figure 6j. The aerogel textile reached an equilibrium surface temperature of ≈130 °C, significantly outperforming conventional cotton and nylon textiles. Improving the mechanical properties of aerogel fibers is also the focus of attention. For example, Liu and co-workers developed the nanoscale Kevlar liquid crystal aerogel fibers with high orientation degrees by combining the liquid crystal spinning and freeze-drying techniques.[105] The synthesis of aerogel fibers comprises liquid crystal spinning, controlled sol-gel transition, freeze drying, and plasma treatment at low temperatures. The obtained Kevlar aerogel fibers revealed an extremely high mechanical strength of 41 MPa attributed to the high orientation of nanofibers. Similarly, Li et al. designed and fabricated the stretchable hierarchical porous PU aerogel fibers based on the regulation of phase separation and NaCl template.[43] The developed PU aerogel fibers exhibited ultrahigh breaking elongation of 816%, higher than the reported porous fiber materials.

Overall, recent advancements in fabrication techniques, such as freeze spinning, have enabled the production of aerogel fibers with outstanding thermal insulating capability. By constructing the core-shell structure or high orientation structure, researchers have further improved the mechanical properties. Aerogel fiber textiles with ultrathin and high thermal retention characteristics are increasingly being explored for applications in extreme environments, including aerospace, military, and outdoor apparel. While significant progress has been made, challenges remain in scaling up production, reducing costs, and enhancing thermal management performance. Future research is expected to focus on optimizing material design, exploring sustainable raw materials, and integrating smart functionalities to address the escalating need for advanced thermal management solutions.

4. Thermally Insulating 3D Micro/Nanofibrous Bulk Materials

Building on the advancements in 2D thermal insulation micro/nanofibrous materials, the exploration of 3D bulk thermal insulation micro/nanofibrous materials represents a natural progression in the pursuit of enhanced thermal management performance. Unlike 2D fibrous membranes and textiles, the 3D bulk materials featured ultralow density, high porosity, and tortuous pathways, which could trap more still air and reduce heat transfer. Recent developments in fabrication techniques, such as the freeze-drying method, direct electrospinning, layer-by-layer stacking, and solution blow spinning, have enabled the design of 3D bulk fiber materials with precise control over their architecture and thermal performance. This section will delve into the design principles, fabrication strategies, and thermal insulation performance of 3D micro/nanofibrous aerogels and sponges.

4.1. Freeze-Drying Method

Freeze-drying has emerged as a versatile and effective technique for fabricating aerogel-based thermal insulation materials with unique structural and functional properties.[106,107] The method can create pores by freezing ice crystals and maintaining the pore structure effectively as the dispersion medium sublimates during drying. By carefully controlling parameters such as freezing temperature, composition, and drying conditions, researchers can optimize the microstructure and performance of the 3D aerogel materials. At present, according to the composition of raw materials, the thermally insulating fiber aerogel is mainly divided into organic and inorganic aerogels. This section explores the advancement of freeze-drying technology in the design of 3D aerogel thermal insulation materials.

In 2014, Si et al. first developed the 3D nanofiber aerogels by incorporating the electrospinning and freeze-drying methods.[108] The fabrication of nanofiber aerogels primarily involves electrospinning, uniform dispersion of nanofibers, freeze-drying, and in situ crosslinking steps. First, the electrospun SiO_2 and PAN/benzoxazine nanofibrous membranes were cut into pieces and introduced into a dispersion solvent, followed by homogenization using a high-speed shear mixer to achieve uniform fiber dispersion. Subsequently, the dispersion was poured into

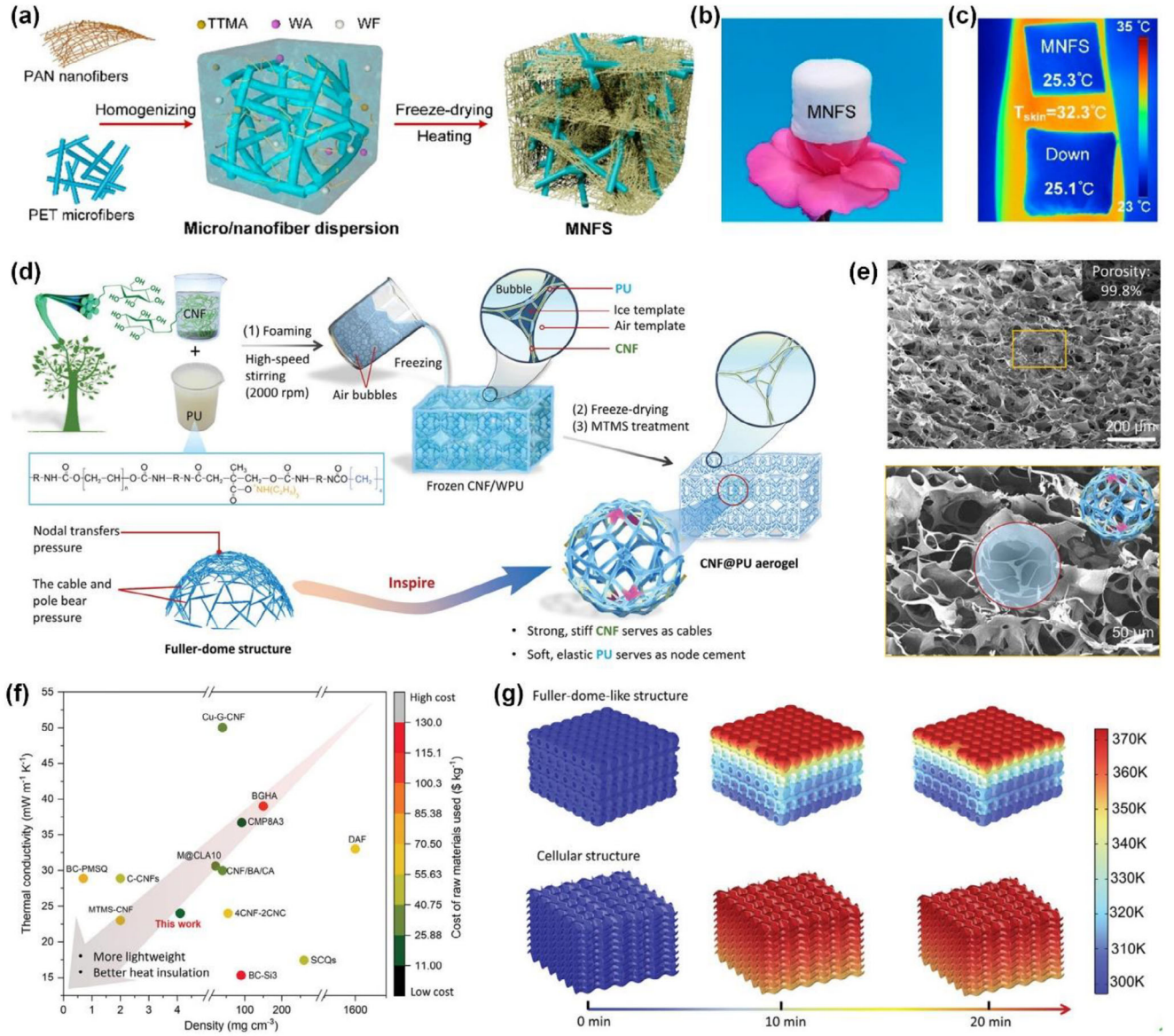

Figure 7. a) Schematic diagram of the synthetic steps for MNFS. b) An optical image illustrating the MNFS standing on the flower. c) The IR image of human skin covered by the down flocculus and MNFS. d) Presentation of the fabrication of the CNF@PU fiber aerogel. e) Microstructure of the CNF@PU aerogel. f) Comparing the thermal insulation performance of different aerogels. g) Analyzing the heat transfer process of aerogel based on the finite element simulation. Reproduced with permission.[109] Copyright 2022, American Chemical Society. Reproduced with permission.[110] Copyright 2024, Wiley-VCH.

a mold and frozen for 10–30 min, and then the frozen sample was transferred to a freeze-dryer. Furthermore, the ultralight and super-elastic 3D fiber aerogels were formed by heating to create adhesive connections between fibers. The fabricated 3D fiber aerogels exhibited adjustable shapes and sizes along with excellent structural flexibility, achieving a remarkably low bulk density of 0.12 mg cm^{-3} and an exceptional porosity of 99.992%. The breakthrough development of such fascinating materials makes them promising candidates for next-generation thermal management materials.

Based on the design concept mentioned above, various polymeric, ceramic, and hybrid nanofiber aerogels were successfully prepared via freeze-drying techniques. For example, Wu and coworkers developed the ultralight, superelastic, and washable micro/nanofibrous aerogels (MNFSs) with rigid-flexible coupled structure via the homogeneous dispersion and freeze-drying method (**Figure 7a**).[109] The high-modulus polyethylene terephthalate microfibers were selected as the rigid skeletons and polyacrylonitrile (PAN) nanofibers served as flexible matrices. As a result, the obtained MNFSs exhibited outstanding resistance to compressive fatigue and superelasticity even at extremely low temperatures (−196 °C). Benefited from the highly porous and tortuous microstructure with nanoscale pores, the MNFSs showed ultralight density (7.5 mg cm^{-3}) and excellent thermal

insulation properties (28.51 mW m^{-1} K^{-1}), matching the insulation capacity of natural down assemblies (Figure 7b,c). To further improve the thermal insulation performance of fiber aerogels, Wang et al. reported a dual-template strategy to fabricate the fuller-dome-structured cellulose/PU (CNF@PU) nanofiber aerogels with low thermal conductivity (Figure 7d).[110] Combining the air template through foaming and the ice template enabled the creation of a dome-like microstructure in the CNF@PU aerogel, which could enhance the phonon scattering effect, resulting in the reduction of heat transfer in the aerogel (Figure 7e). Compared with the reported cellulose-based aerogels (>30 mW m^{-1} K^{-1}), the CNF@PU aerogel exhibited excellent heat insulation capability with a low thermal conductivity of 24 mW m^{-1} K^{-1} (Figure 7f,g). Although the nanofiber aerogels presented satisfactory thermal management performance, the inherent brittleness of porous skeletons makes them prone to fail under extreme forces. Therefore, Wu et al. proposed the multi-scale toughening strategy by processing the aramid nanofibers into tough 3D aerogel monoliths.[111] The dense skeletons formed by highly aggregated nanofibers imparted the aerogels with a remarkable specific tensile strength of 89 MPa cm^3 g^{-1}, ultra-high toughness of 1.3 MJ m^{-3}, and outstanding fracture energy of 7.36 kJ m^{-2}. Besides, the aligned sheets in the aerogels enabled the superior thermal conductivity of 15.8 mW m^{-1} K^{-1}. Considering the effect of relative humidity on the thermal insulation property, Di and co-workers prepared the super-insulating aerogels composed of acid-treated aramid nanofibers and tempo-oxidized cellulose nanofibers.[112] The resulting hybrid aerogels displayed low thermal conductivity even at a wide relative humidity range of 20% to 80%. To enhance the preparation efficiency, Li et al. presented a versatile ice-templating method that involves freezing the material on a rotating cryogenic drum, fragmenting treatment, and subsequently freeze drying.[113] The aerogel production was easily scaled up, achieving an area exceeding 1.2 m^2. Such large-area nanofiber-based aerogel has rarely been reported.

Although organic fiber-based aerogels have demonstrated exceptional thermal insulation properties, ultralight characteristics, and tunable mechanical strength, their practical applications are often limited by inherent challenges such as flammability and thermal instability at extreme temperatures.[65,83] Therefore, researchers have increasingly turned to inorganic fiber-based aerogels, which leverage materials like silica, alumina, and ceramic fibers. These inorganic fiber aerogels offer superior thermal stability, fire resistance, and robustness in harsh environments, making them ideal for high-temperature insulation applications.[46] The routine procedure for the fabrication of inorganic micro/nanofiber aerogels includes the preparation of inorganic micro/nanofiber based on the sol-gel electrospinning method, homogeneous dispersion of nanofibers, freeze-drying of dispersions, and calcination. Based on the strategy, in 2018, Si et al. reported ceramic nanofibrous aerogels with a lamellar architecture by integrating SiO_2 nanofibers into aluminoborosilicate matrices (**Figure** 8a).[47] As illustrated in Figure 8b, the resulting ceramic aerogels demonstrated excellent thermal insulation performance when exposed to a high-temperature butane blowtorch flame, maintaining a remarkably low temperature of 35 °C on the opposite side. Additionally, the aerogels showcased ultralight densities exceeding 0.15 mg cm^{-3} and maintained superelasticity without degradation even at temperatures up to 1100 °C. The innovative ceramic design provides transformative opportunities for next-generation high-temperature insulation systems. However, the inherent fragility of current ceramic aerogels leads to immediate structural failure under slight deformation (<5% strain), precluding applications requiring mechanical flexibility. Therefore, Dou and co-workers introduced a versatile approach to preparing ceramic nanofibrous aerogels with exceptional flexibility and compressibility, achieved by assembling flexible SiO_2 nanofibers with a high aspect ratio into a robust and interconnected cellular framework.[50] As shown in Figure 8c, the SEM images revealed the fibrous cellular networks composed of SiO_2 nanofibers that are intricately interconnected, forming a seamless and interwoven cellular architecture. The stable junctions between cells would greatly enhance the integrity and flexibility of the aerogel. Excitingly, the developed aerogels demonstrated significant recovery from compression and buckling strains (85%), exceptional fatigue resistance enduring up to 100 000 cycles, and low thermal conductivity of 22.3 mW m^{-1} K^{-1}. Similarly, Zhang et al. fabricated the superelastic amorphous SiC aerogels by constructing the strong binding structure within the resilient nanofiber skeleton network.[114] The innovation point derives from the controlled establishment of a covalently cross-linked network, accomplished through rheological manipulation of AlBSi sols on hydrophobic nanofiber surfaces and subsequent interfacial coupling. The resulting SiC aerogel presented temperature-invariant superelasticity, resistance to fatigue with minimal permanent deformation of 5% after 1000 compression cycles, and ultralow thermal conductivity of 19 mW m^{-1} K^{-1}. To further enhance the mechanical properties, Liu et al., inspired by the reinforced concrete building envelope, designed the interlocked fibrous interfaces and a cellular structure interwoven in orthogonal directions.[115] The manufacturing of the ceramic aerogel involved fiber-based framework assembly, supramolecular arrangement, and mineral deposition. Remarkably, the maximum stress of the fabrication BN/C/Al_2O_3 ceramic aerogel reached 11.3 kPa at 60% strain, indicating that the aerogel could endure loads up to 6000 times its own weight without fracturing (Figure 8d). Interestingly, the aerogel with a volume of 2 cm^3 could be compressed to cross a thin pipe with a diameter of 0.5 cm, demonstrating superior mechanical robustness (Figure 8e). Moreover, the aerogels demonstrated outstanding adaptability for thermal shock resistance and infrared camouflage performance in cold (−196 °C) and hot (1300 °C) environments (Figure 8f,g). In addition to improving the mechanical strength, few works focus on the study of enhancing the heat-resistance temperature of the aerogels. For example, Chang et al. fabricated the mullite-carbon hybrid nanofibrous aerogels with the multiphase sequence and multiscale structure.[116] The key innovation involves combining carbon-reinforced mullite-like ceramic nanoparticles with 1D nanofibers, followed by their hierarchical assembly into resilient 3D aerogels possessing a laminated cellular framework. The synergistic interaction between the components effectively suppresses both ceramic crystalline coarsening and carbon thermal degradation, thereby ensuring thermal stability. Eventually, the ceramic-carbon aerogels exhibited thermomechanical stability under extreme aerobic environments up to 1600 °C.

In summary, the freeze-drying method has emerged as a versatile and effective technique for fabricating organic and inorganic

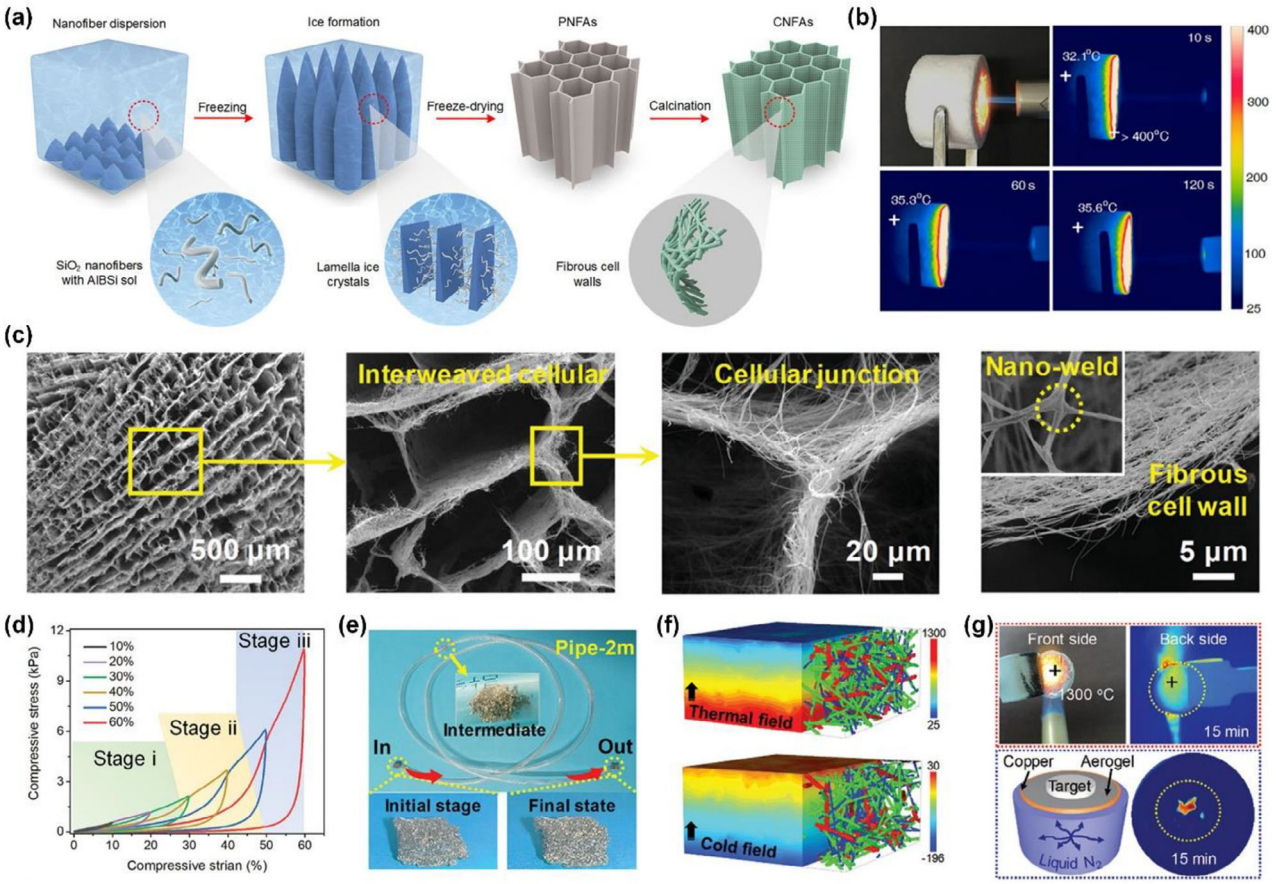

Figure 8. a) Schematic illustration of the synthetic steps of CNFAs. b) Optical and IR images of CNFAs after exposure to the butane blowtorch. c) SEM images of the ceramic nanofibrous aerogels at different magnifications. d) The compressive stress-strain curves of the BN/C/Al_2O_3 ceramic meta-aerogel. e) The deformation test of the ceramic meta-aerogel. f) Simulated the heat transfer process of the aerogel. g) Optical and IR images illustrating the temperature distribution of the meta-aerogel heated at 1300 °C or frozen at −196 °C. Reproduced with permission.[47] Copyright 2018, AAAS. Reproduced with permission.[50] Copyright 2020, Wiley-VCH. Reproduced with permission.[115] Copyright 2024, Wiley-VCH.

micro/nanofiber aerogels with exceptional thermal insulation properties. By utilizing ice crystals as templates, this technique enables the production of lightweight, highly porous, and structurally robust materials. Despite these advancements, challenges remain in achieving large-scale production with consistent quality, further reducing thermal conductivity, and enhancing mechanical durability under dynamic stress. Addressing these challenges will pave the way for the development of next-generation thermal insulation materials tailored for applications in energy-efficient buildings, aerospace, and extreme environments.

4.2. Direct Electrospinning

Direct electrospinning techniques have emerged as a promising technique for fabricating 3D bulk micro/nanofiber sponges with exceptional thermal insulation properties. Unlike traditional electrospinning, which typically produces 2D nanofibrous membranes with dense lamellar structure, this advanced approach enables the creation of lightweight, highly porous, and hierarchically structured materials with enhanced thermal management capabilities. By optimizing parameters such as solution viscosity, solvent evaporation rate, and collector design, direct electrospinning allows for the precise control of fiber morphology and spatial arrangement, resulting in materials with ultralow thermal conductivity and superior mechanical flexibility. This section explores the principles, advancements, and thermal performance of 3D micro/nanofiber sponges fabricated via direct electrospinning, highlighting their unique advantages and prospects in the field of thermal insulation.

At present, the micro/nanofiber thermal insulation sponges based on the direct electrospinning method mainly include two types: polymer-based micro/nanofiber sponges and ceramic micro/nanofiber sponges. The preparation process of polymer-based micro/nanofiber sponges involves selecting the unique polymer, preparing a homogeneous polymer solution, optimizing electrospinning parameters (e.g., collector distance, spinning temperature, spinning humidity), and heat treatment. Up to now, some researchers believe that the formation mechanism of the sponges with fluffy structures depends on the rapid phase separation of the spinning jet at high relative humidity. The faster phase separation in the system resulted in the generation of rigid fiber with large diameters, thus providing enough strength to maintain the 3D structure of the sponges. So far, some poly-

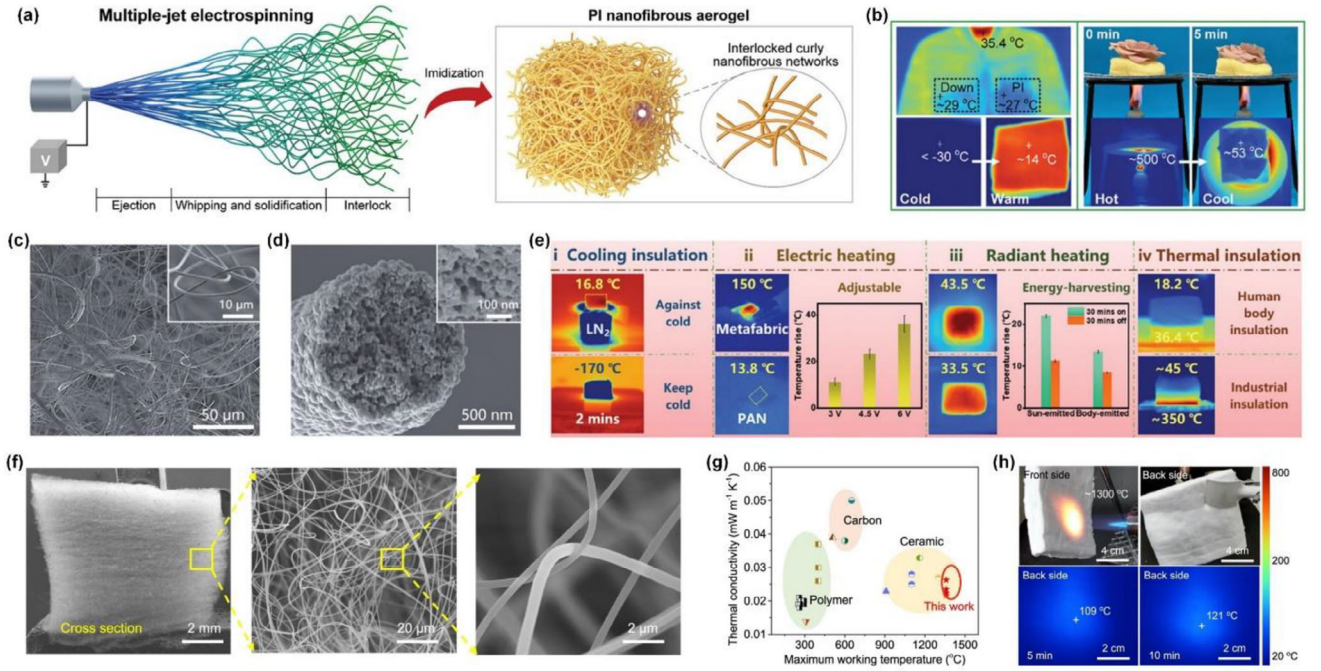

Figure 9. a) Presentation of fabricating the PI nanofibrous sponge. b) Optical and IR images of the sponge in high-temperature and cold environments. c,d) SEM images of the metafabric. e) Various thermoregulation methods of the metafabric. f) SEM images of ceramic nanofiber sponges. g) Comparison of the thermal conductivity and maximum operational temperature of various thermal insulation materials. h) Optical and infrared thermal images depict ceramic sponges subjected to a butane blowtorch flame for 10 min. Reproduced with permission.[51] Copyright 2024, Wiley-VCH. Reproduced with permission.[119] Copyright 2024, Wiley-VCH. Reproduced with permission.[35] Copyright 2022, Springer Nature.

mers, such as polystyrene (PS), polysulfone (PSU), polyphenylene sulfone (PPSU), and PI have been explored to fabricate the 3D sponges.[18] In 2012, Lin et al. first reported the fabrication of 3D PS fibrous sponges by tuning the solvent compositions.[117] However, the structure of the PS sponge collapses easily under the action of external forces, resulting in limited application in the thermal insulation field. To solve the problem, Wu and co-workers proposed a facile strategy to fabricate the ultralight and mechanically robust warmth retention sponges by constructing stiff-soft polymer networks within fibers and bonding architecture among fibers based on direct electrospinning and thermal crosslinking.[118] The stiff PS could impart the sponges with structural rigidity, and soft PU could facilitate energy absorption during deformation. Eventually, the fabricated fibrous sponges demonstrated remarkable elongation at a break of 70%, excellent resilience withstanding 100 compression cycles at 50% strain even at −50 °C, and efficient thermal insulation performance with a low thermal conductivity (27.6 mW m^{-1} K^{-1}). In addition to improving the mechanical properties, some researchers focused on enhancing the temperature resistance and warmth retention of the micro/nanofibrous sponges. For example, Wang et al. synthesized the thermally insulating PI fibrous sponges by creating 3D interlocking networks of curly nanofibers during electrospinning (**Figure 9a**).[51] The interaction between the jets and water molecules was precisely controlled to facilitate the phase separation of the charged jet into curly nanofibers, thus facilitating the formation of a 3D structure. As a result, the PI nanofibrous sponges exhibited exceptional temperature resilience and mechanical stability across a broad temperature range from −196 to 300 °C. Additionally, the sponge demonstrates outstanding thermal insulation capabilities with a low thermal conductivity of 22.3 mW m^{-1} K^{-1}, effectively minimizing heat transfer with the surrounding environment (Figure 9b). However, the micro/nanofiber sponges only rely on porous structures to prevent heat diffusion, resulting in inadequate thermal performance in extreme environments. Integrating adjustable active thermal regulation with effective passive radiation absorption capabilities would solve the above bottleneck problem. A typical example is the fabrication of a carbon fiber sponge based on direct electrospinning and carbonization treatment.[119] The charge density of the solution and PAN/water interaction was manipulated to enhance the coulombic repulsion and phase separation rate, resulting in the generation of curly nanofibers with internal nanopores (Figure 9c,d); and then, the carbon nanofiber sponges were prepared by pre-oxidation and graphitization. As depicted in Figure 9e, the carbon sponges metafabric exhibited the ability to dynamically modulate its thermal properties in alignment with environmental conditions. The sponges could sustain stable temperatures for 2 min after absorbing liquid nitrogen, demonstrating exceptional cooling insulation capabilities. More importantly, the sponges could be heated by a direct-current source and sunlight, illustrating the superior electrothermal, photothermal, and passive warming performance.

Polymer-based micro/nanofibrous sponges have demonstrated excellent thermal insulation properties, lightweight characteristics, and mechanical flexibility. However, the sponges often face limitations in extreme environments, such as high temperatures or corrosive conditions, due to their relatively low thermal

stability and mechanical degradation under prolonged thermal or chemical exposure. To address these challenges, researchers have shifted focus toward ceramic-based micro/nanofibrous sponges, which offer superior thermal stability, fire resistance, and mechanical robustness at elevated temperatures. In 2022, Cheng and co-workers first synthesized ceramic nanofibrous sponges with 3D interwoven crimped nanofiber structures by reaction electrospinning.[35] The fabrication process of ceramic sponges mainly includes the preparation of mullite sol, direct electrospinning, and calcination. The gelation rate of the sol jet was finely regulated by adjusting the protonation degree of colloidal particles, enabling the production of crimped nanofiber (Figure 9f). In comparison to previously reported high-performance ceramic insulators, the ceramic micro/nanofiber sponges exhibited the lowest thermal conductivity of 0.0228 W m^{-1} K^{-1} and exceptional structural stability at temperatures up to 1400 °C (Figure 9g,h). Based on the design concept, a series of inorganic nanofiber sponges have been synthesized, including TiO_2, $CaCu_3Ti_4O_{12}$, $SrTiO_3$, In_2TiO_5, etc.[120] The successful development of such high-performance inorganic sponges has laid a solid foundation for the next generation of thermal protection systems in space vehicles.

In summary, direct electrospinning has proven to be a highly effective method for fabricating 3D micro/nanofibrous thermal insulation sponges. By enabling precise control of precursor solution, spinning condition, and post-processing, the organic or inorganic micro/nanofibrous sponges with lightweight, superelastic, and high warmth retention could be obtained. However, challenges such as scalability, mechanical strength, and long-term stability under harsh conditions remain to be addressed. Future research should focus on overcoming these limitations while exploring innovative material combinations to further advance the performance and applicability of the 3D fibrous sponges in thermal insulation.

4.3. Layer-by-Layer Stacking

The layer-by-layer stacking of micro/nanofibers membranes into 3D aerogel structures has emerged as an innovative approach to designing high-performance thermal insulation materials.[121] In contrast to the 3D bulks by freeze-drying or direct electrospinning method depending on intermittent fiber segment connectivity, the nanofibrous aerogels based on the layer-by-layer stacking possessed the lamellar multi-arched cellular structure, presenting robust compressive strength and deformation resistance under high-stress loading. This section delves into the fabrication techniques, structural innovations, and thermal performance of the layered aerogels.

In 2020, Zhang and co-workers first reported the lamellar multiarch structured ZrO_2-Al_2O_3 nanofibrous aerogels.[122] The fabrication process of the aerogels mainly included the preparation of precursor solution, electrospinning, lamellar stacking in the solution of the binding agent, and calcination (**Figure 10a**). First, the ZrO_2-Al_2O_3 precursor solution was prepared via the sol-gel method, and then fabricated the ZrO_2-Al_2O_3 membranes by electrospinning and calcination treatment. Subsequently, the membranes were cut into squares and stacked in layers in aqueous solution of binding agent. Furthermore, the stacked membranes were freeze-dried and calcined to prepare 3D laminar nanofibrous aerogels. As shown in Figure 10b, the obtained ZrO_2-Al_2O_3 aerogels (ZrAlNFAs) with 1 cm thickness could effectively protect fresh flowers from dehydration, fading, and carbonization even when exposed to a butane blowtorch for over 5 min, demonstrating satisfactory fire resistance and thermal insulation performance. Inspired by the reported layer-by-layer stacking method, some work has been done to enhance the thermal insulation. Incorporating the aerogel nanoparticles and nanosheets into the lamellar multi-arched cellular structured aerogels would reduce the heat diffusion, improving the thermal insulation performance. A typical example was the design and fabrication of hierarchically structured ceramic aerogel with multi-arch cellular and biomimetic leaf-vein network morphologies.[123] As depicted in Figure 10c, the cross-sectional SEM images of the aerogels revealed a hierarchical cellular architecture, featuring lamellar arch-shaped cells, nanofibrous walls embedded with silica granular aerogels (SGAs), and interconnected bonding regions between the fibers and SGAs. Attributed to the thermal insulation capabilities of SGAs and the flame-retardant character of the ceramic elements, the composite aerogels demonstrated exceptional thermal insulation performance, achieving a thermal conductivity as low as 0.024 W m^{-1} K^{-1} while maintaining remarkable resistance to high temperatures (1100 °C, Figure 10d). Similarly, Li et al. prepared the quasi-ordered mullite fiber aerogels via doping the SiO_2 aerogels into the mullite fiber layer based on the fiber sedimentation and layer-by-layer assembly strategy.[124] Eventually, the fabricated aerogels exhibited the integrated properties of low thermal conductivity (0.034 W m^{-1} K^{-1}) and temperature-invariant compression resilience from −196 to 1300 °C.

In addition to thermal insulation properties, the mechanical properties of aerogel are also widely considered by researchers. After millions of years of survival, most of the creatures that survive in nature have evolved unique structures and functions. Shell nacre is a kind of brick and mud structure composed of soft and hard material layers, which makes the shell have high strength and toughness; mantis shrimp knuckles are a unique plywood spiral arrangement structure, which can effectively alleviate the external mechanical impact.[125] Inspired by the nature structure, Wang et al. introduce an innovative approach that integrates compositional and structural engineering, leveraging macro/nanoscale manipulation of building blocks alongside precise geometric design in helical chiral fiber arrays.[46] This strategy facilitates the simultaneous creation of ceramic fibrous aerogels with tailored properties. Remarkably, the tensile strength of the biomimetic ceramic aerogels reached an impressive 170.38 MPa, surpassing the cutting-edge nanofiber aerogels by one to two orders of magnitude. Moreover, the ceramic aerogels could withstand pressures of up to 156.47 kPa at 80% strain, demonstrating exceptional compressive resilience. However, as space and planetary exploration advance, the extreme and unpredictable environmental conditions, characterized by drastic temperature fluctuations, impose increasingly demanding criteria for thermal protection systems, especially for mechanical durability. Apparently, the common aerogels suffered from poor tensile elasticity, resulting in limited application in spacesuits and hypersonic spacecraft. To solve the bottleneck problem, Zhang et al. proposed a programmable

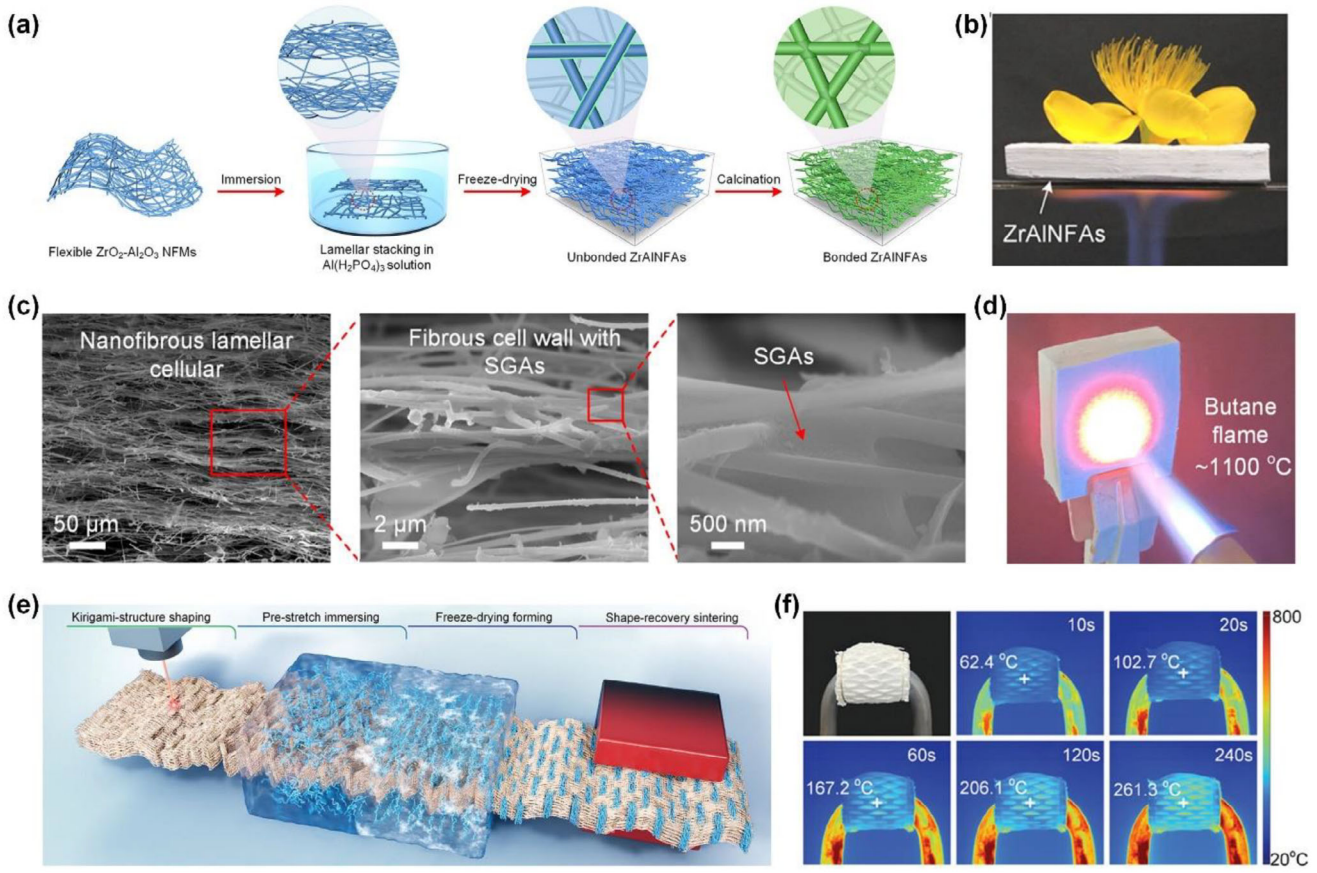

Figure 10. a) The construction steps of lamellar nanofibrous aerogels. b) Demonstration of thermal insulation property of ZrAlNFAs. c) The microstructure of ZNGAs. d) ZNGA maintains intact and undamaged when exposed to the flame of a butane blowtorch. e) Thermal insulation mechanism of aerogels. f) The fabrication process of the kirigami lamellated aerogels. g) Optical and IR images of a butane nozzle protected by ceramic aerogels. Reproduced with permission.[122] Copyright 2020, American Chemical Society. Reproduced with permission.[123] Copyright 2022, American Chemical Society. Reproduced with permission.[126] Copyright 2024, Wiley-VCH.

shape-morphing strategy to develop ceramic aerogels.[126] The fabrication process of the kirigami lamellated aerogels includes shaping the kirigami structure, immersing with pre-stretching, followed by freeze-drying, and finally sintering (Figure 10e). The unique topological architecture, featuring kirigami-inspired laminated aerogels to bear compressive stress and randomly arranged aerogels for pre-storing mechanical energy to transfer tensile stress, effectively achieves robust mechanical tensile performance and thermal stability. As a result, the obtained aerogels exhibited remarkable mechanical fatigue resistance, enduring 1,000 cycles at 60% buckling strain and 500 cycles at 50% compressive strain without significant degradation. Besides, the aerogels presented remarkable elasticity even when exposed to flames at 1100 °C and low thermal conductivity of 33.01 mW m^{-1} K^{-1} (Figure 10f).

In summary, the layer-by-layer stacking method is an effective technique for fabricating micro/nanofiber aerogels with structural robustness and excellent heat barrier properties. This approach enables precise control over the structural hierarchy, porosity, and density of the aerogels by sequentially assembling 2D fibrous membranes into 3D interconnected networks. Moreover, the methods allow for the incorporation of functional additives or structural design during assembly, enhancing properties such as mechanical strength, fire resistance, and warmth retention. Although there has been considerable progress in layer-by-layer stacking aerogels, several limitations hinder their widespread application. First, the assembling process is often time-consuming, requiring multiple steps to achieve the desired structural integrity and performance. Second, achieving a uniform distribution of fiber layers and strong interfacial bonding between layers remains challenging. Additionally, scalability is a significant concern, however, the method is difficult to adapt for large-scale production. Addressing these challenges through process optimization, advanced bonding strategies, and scalable manufacturing techniques will be critical for advancing the practical application of layer-by-layer stacking micro/nanofiber aerogels in thermal insulation.

4.4. Solution Blow Spinning

Solution blow spinning, an innovative and scalable micro/nanofiber fabrication technique, has recently gained significant attention for producing 3D bulk fiber sponges

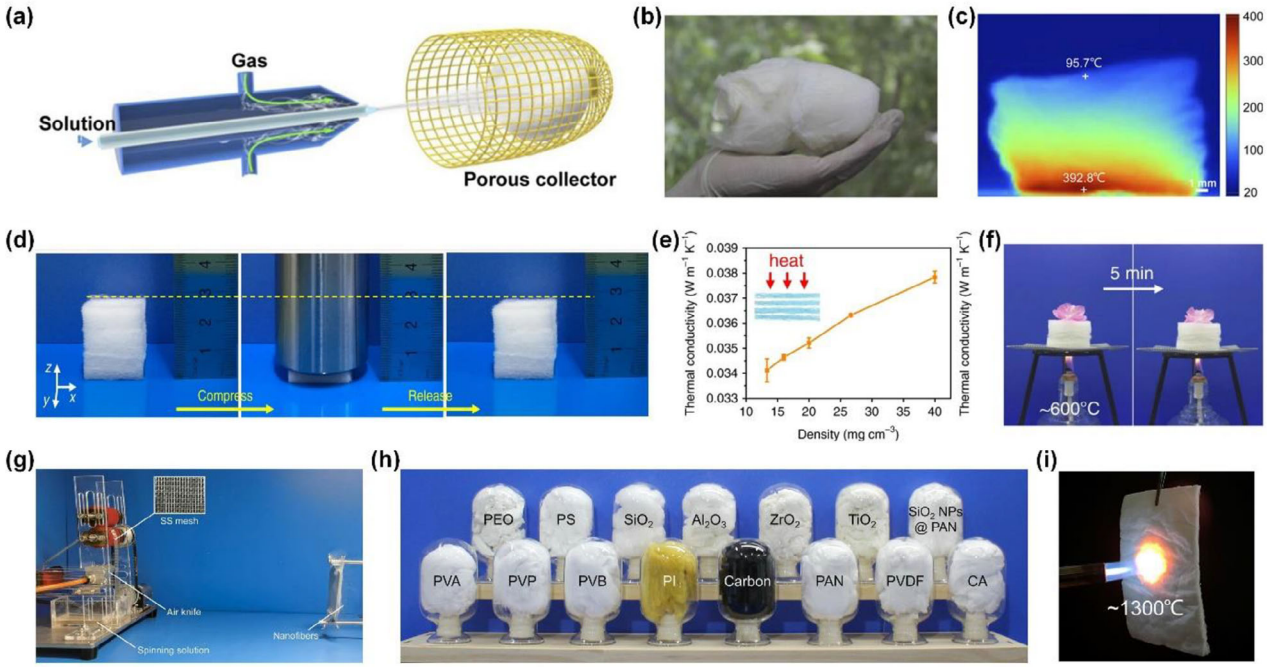

Figure 11. a) Schematic diagram of solution blow-spinning technique. b) Photograph of a macro-sized sponge. c) IR image of ZrO_2 sponge heated by hot stage. d) Compression and release of the ceramic sponge. e) Thermal conductivity of the ceramic sponge. f) Demonstration of thermal insulation property of the sponge. g) Photograph of the solution blow-spinning system. h) Pictures of a variety of nanofiber sponges. i) A photograph illustrating the fire resistance of the SiO_2-Al_2O_3 sponge. Reproduced with permission.[127] Copyright 2017, AAAS. Reproduced with permission.[33] Copyright 2020, Springer Nature. Reproduced with permission.[129] Copyright 2022, AAAS.

with lightweight and highly porous characteristics. By leveraging high-speed airflow to stretch and deposit micro/nanofibers into 3D bulk materials, this technique offers precise control over fiber diameter, porosity, and spatial arrangement, which are critical for optimizing thermal insulation performance. This section explores the principles, advantages, and potential of solution blow spinning in fabricating 3D micro/nanofiber sponges, highlighting their unique structural features and performance in thermal insulation.

In 2017, Wang et al. first reported the fabrication of lightweight 3D ceramic micro/nanofiber sponges via an effective solution blow-spinning technique.[127] The manufacturing process of the ceramic sponges is mainly involved in the preparation of precursor solution, stretching the solution into micro/nanofibers by the airflow, and high-temperature calcination (**Figure 11a**). When the precursor contains a high concentration of inorganic salts, a jamming effect often occurs near the syringe needle tip during electrospinning. In contrast, blow-spinning enables the effortless processing of precursors containing high concentrations of inorganic salts. Therefore, the blow-spinning method presented a universal method for preparing various ceramic fiber sponges, such as TiO_2, SiO_2, and $BaTiO_3$. Moreover, the approach was not only highly efficient but also easily scalable, enabling the rapid production of a large ceramic nanofiber sponge (Figure 11b). Benefited from the highly porous structure, the IR image in Figure 11c demonstrates that the surface of the ceramic nanofiber sponges remained at a relatively low temperature of ≈95 °C after being exposed to a 400 °C heating stage for 1 h, highlighting the exceptional thermal insulation properties.

Based on the design strategy of blow-spinning, a series of subsequent research was carried out, mainly focusing on enhancing the thermal insulation, reducing the fiber diameter, and improving the production rate. For example, Jia and co-workers proposed a straightforward approach for fabricating compressible and thermal-resistant SiO_2-Al_2O_3 composite ceramic sponges through blow spinning followed by calcination.[33] Significantly, as shown in Figure 11d, the ceramic sponge fully recovered its initial shape with no noticeable dimensional alteration after removing the pressure, showcasing exceptional compressibility. Gained from the layered structure and multi-phase ceramic composition, the micro/nanofiber sponge exhibited temperature-invariant compression resilience from −196 to 1000 °C and low thermal conductivity of 0.034 W m^{-1} K^{-1} (Figure 11e,f). To reduce the fiber diameter, Cao et al. proposed the electro-blown spinning method that combines the electric field with high-speed gas flow to stretch polymer solutions into ultrafine fibers.[128] The average fiber diameter based on electro-blown spinning can be adjusted to ≈454 nm, significantly lower than the fiber diameter (≈613 nm) of blow spinning. For the solution blow spinning, researchers are also constantly concerned about the mass production of nanofibers. At present, only needle-based solution blow spinning methods have been reported, which exhibit limited production throughput. Therefore, researchers focus on the needleless solution of blow spinning to solve the problem mentioned above. A typical example was the development of the needleless Kármán vortex solution blow spinning system, which employs a roll-to-roll nylon thread to supply the spinning solution, combined with vertically directed airflow to efficiently produce

high-quality nanofibers (Figure 11g).[129] As a result, the nanofiber production rate of the spinning system could reach 5.9 g/h/per jet, higher than the traditional electrospinning methods. Benefited from the versatility of the method, diverse nanofibrous sponges could be fabricated, such as PI, PVDF, PAN, cellulose acetate, polyvinyl pyrrolidone, carbon, and ceramics (Figure 11h). The prepared ceramic could withstand the 1300 °C flame of a butane blowlamp, exhibiting excellent high-temperature resistance (Figure 11i).

In summary, solution blow spinning has proven to be a highly effective and scalable method for fabricating thermally insulating micro/nanofiber sponges. Attributing to the high porosity and hierarchical porous structures, the 3D sponges exhibit exceptional thermal insulation properties. These characteristics, combined with the controlled preparation of various organic, inorganic, and composite nanofibers, make the sponges versatile for applications ranging from energy-efficient buildings to advanced textiles. While significant progress has been made, further research is needed to optimize production parameters, enhance mechanical durability, and explore eco-friendly materials to meet the growing demand for sustainable and high-performance thermal insulation.

5. Applications of Micro/Nanofibrous Thermal Insulation Materials

Generally, the advancement of novel materials has consistently followed a trajectory of foundational research and functional innovation.[130] Over the last 10 years, the development of micro/nanofibrous thermal insulation materials has laid a solid foundation for various applications attributed to the lightweight, high porosity, and excellent thermal management properties. From personal thermal comfort in clothing to high-technology applications in aerospace and automotive industries, as well as energy-efficient building, fiber-based thermal insulation materials play a pivotal role in addressing modern thermal management challenges.[27,96] This section explores the diverse applications of micro/nanofiber thermal insulation materials, highlighting their significance and adaptability in fields such as personal warming equipment, aerospace engineering, automobile industry, and sustainable building.

5.1. Personal Warming Equipment

Micro/nanofiber thermal insulation materials have revolutionized the field of personal thermal clothing, offering unparalleled warmth and comfort while maintaining lightweight and flexible properties.[131] These advanced materials leverage unique structural characteristics, such as high porosity, low thermal conductivity, and excellent breathability, to create garments that effectively retain body heat in cold environments. This section explores the key advancements and applications of micro/nanofiber thermal insulation materials in personal protective equipment, highlighting their role in enhancing thermal comfort and energy efficiency for individuals.

Since the emergence of humankind, clothing, food, shelter, and transportation have been essential for survival and daily living.[132] Among these, thermally insulating fabrics play a critical role in maintaining body temperature and ensuring thermal comfort in extreme weather conditions. According to the latest report forecasts, the thermal insulated coat market reach ed $207.2 billion by 2024.[133] Generally, natural fibers such as cotton, silk, wool, and down feathers have long been processed and employed in the production of thermal garments to minimize heat loss from the human body. Nevertheless, their limitations, including relatively large fiber diameters (typically >20 µm) and a tendency to absorb moisture, restrict their effectiveness in minimizing heat transfer.[18,51] Advancements in science and technology have led to the creation of numerous synthetic fibers, characterized by smaller diameters, hydrophobic properties, and enhanced thermal insulation capabilities, designed to meet diverse application needs. Research into the application of micro/nanofiber thermal insulation materials in cold-proof clothing is summarized in **Table 1**. For example, Wu et al. fabricated a warmth retention sweater made of encapsulated aerogel fiber based on traditional knitting techniques. Interestingly, the surface temperature of the aerogel fiber textile (3.5°) was lower than the down jackets (3.8°), wool (7.2°), and cotton sweaters (10.8°), demonstrating superior thermal insulation efficiency.[104] The advanced ultrathin aerogel textiles boast exceptional thermal insulation properties and versatile functionality, making them highly suitable for applications in military gear and space exploration suits.

The wearer with aerogel textiles can enjoy good warmth without increasing the thickness of the clothing while maintaining the flexibility of movement. However, in extremely cold environments, 2D aerogel textiles may still encounter certain challenges. The primary reason is that the thickness of the functional textiles is typically thin, which somewhat limits their thermal insulation capabilities. Additionally, in high-wind conditions, the rate of heat loss increases significantly. In comparison, the 3D micro/nanofiber aerogels or sponges possess hierarchical structure and high porosity, thus providing excellent thermal insulation performance in extreme climates.[46,118] For example, Wang and co-workers developed a lightweight and mechanically robust sponges made from curly wrinkled PS/PU micro/nanofiber via direct electrospinning (**Figure 12**a,b).[137] Benefiting from the high porosity of 99.3%, the resultant sponges exhibited satisfactory warmth retention performance with thermal conductivity of 24.5 mW m^{-1} K^{-1}. Meaningfully, the sponges can be made into practical clothing to prevent heat from spreading through the body, as presented in Figure 12c. Compared with the down feather filling with high-level warmth retention performance, the thermal imaging results indicated that the PS/PU micro/nanofiber sponges showed lower surface temperature, illustrating that the sponges effectively retained more heat (Figure 12d). This novel technique establishes an effective foundation for the preparation of fluffy micro/nanofiber sponges. Similarly, Yu et al. employed sea-island melt-spun ultrafine fibers to construct a 3D aerogel characterized by an interwoven wrinkled lamellar architecture based on the freeze-drying method (Figure 12e,f).[140] The resulting ultrafine fibrous aerogels exhibited a lightweight of 6.4 mg cm^{-3}, robust mechanical flexibility with over 25% tensile strain, and low thermal conductivity of 28 mW m^{-1} K^{-1}. Attributed to the mechanical robustness, the ultrafine fibrous aerogels could be processed into interlining to enhance the warmth of outwear.

Table 1. Comparison of properties of the thermal insulation materials.

Material	Morphology	Porosity [%]	Tensile stress [MPa]	Thermal conductivity [mW m^{-1} k^{-1}]	Thermal conductivity evaluation method	Refs.
PVDF/AgNWs	2D membrane	84	3.6	18	Transient plane source technique	[41]
PMMA/CB	2D membrane	91.3	2.12	15.8	Transient plane source technique	[40]
PS/PA6	2D membrane	91.2	0.625	14.01	Transient plane source technique	[36]
Silk fibroin	2D textile	87	0.95	21.86	Transient plane source technique	[31]
Zylon	2D textile	98.6	8.6	36	Transient hot wire method	[42]
Chitosan/TPU	2D textile	90	12.7	26.9	Transient plane source technique	[104]
Silica/aramid	2D textile	/	3.4	33	Transient hot wire method	[134]
PI	2D textile	88.9	11	32	Heat flow meter	[135]
PI/$Ti_3C_2T_x$	2D textile	/	26	36	Transient plane source technique	[136]
PI	2D textile	88	14.7	36.4	Transient plane source technique	[99]
PI/PVA	2D textile	95.6	5.2	28.7	Transient plane source technique	[100]
PU/PSU	3D sponge	99.8	1	25.8	Transient plane source technique	[45]
PS/PU	3D sponge	99.31	0.367	27.6	Transient plane source technique	[118]
PU/PPSU	3D sponge	99.5	0.148	24.6	Transient plane source technique	[49]
PS/PU	3D sponge	99.3	/	24.5	Transient plane source technique	[137]
PI	3D sponge	99.8	0.278	22.4	Transient plane source technique	[51]
PEI/MXene	3D sponge	99.5	0.065	24.6	Transient plane source technique	[138]
PS/PU	3D sponge	99.7	/	25.3	Transient plane source technique	[139]

Significantly, the aerogel clothing achieved comparable insulation performance to down while being only one-third the thickness (Figure 12g). To optimize the thermal insulation performance of aerogel clothing, Wang and co-workers reported the superhydrophobic fuller-dome-structured cellulose nanofiber aerogels with thermal conductivity of 24 mW m^{-1} K^{-1}.[110] As illustrated in Figure 12h–j, the outer surface temperature of the jacket with cellulose nanofiber aerogels (9 mm in thickness) was solely 9.2 °C, significantly lower than the flannelette clothing (17.3 °C, 9 mm) and goose down clothing (10.4 °C, 40 mm). This demonstrates that the aerogel filler possesses significantly superior thermal retention performance compared to conventional commercial insulating clothes.

In conclusion, the micro/nanofiber thermal insulation materials have demonstrated remarkable potential in personal warming equipment. Their lightweight, exceptional thermal insulation properties, and flexibility make them highly suitable for meeting the demands of modern wearable technologies. These advanced materials not only enhance thermal comfort but also contribute to energy efficiency by reducing heat loss. As research progresses, further improvements in durability, breathability, and scalability are expected, paving the way for broader adoption of cold-proof apparel as well as specialized protective fabrics.

5.2. Aerospace Industry

The application of micro/nanofiber thermal insulation materials in the aerospace field represents a critical advancement in addressing extreme thermal challenges. Aerospace systems, including spacecraft, satellites, and high-altitude aircraft, operate in environments characterized by severe temperature fluctuations, ranging from intense solar radiation to the extreme cold of outer space.[61] Traditional insulation materials often fall short of meeting the stringent requirements of lightweight, high thermal resistance, and durability under such conditions.[65] Micro/nanofiber thermal insulation materials, with their unique structural properties and exceptional thermal performance, have emerged as a promising solution.

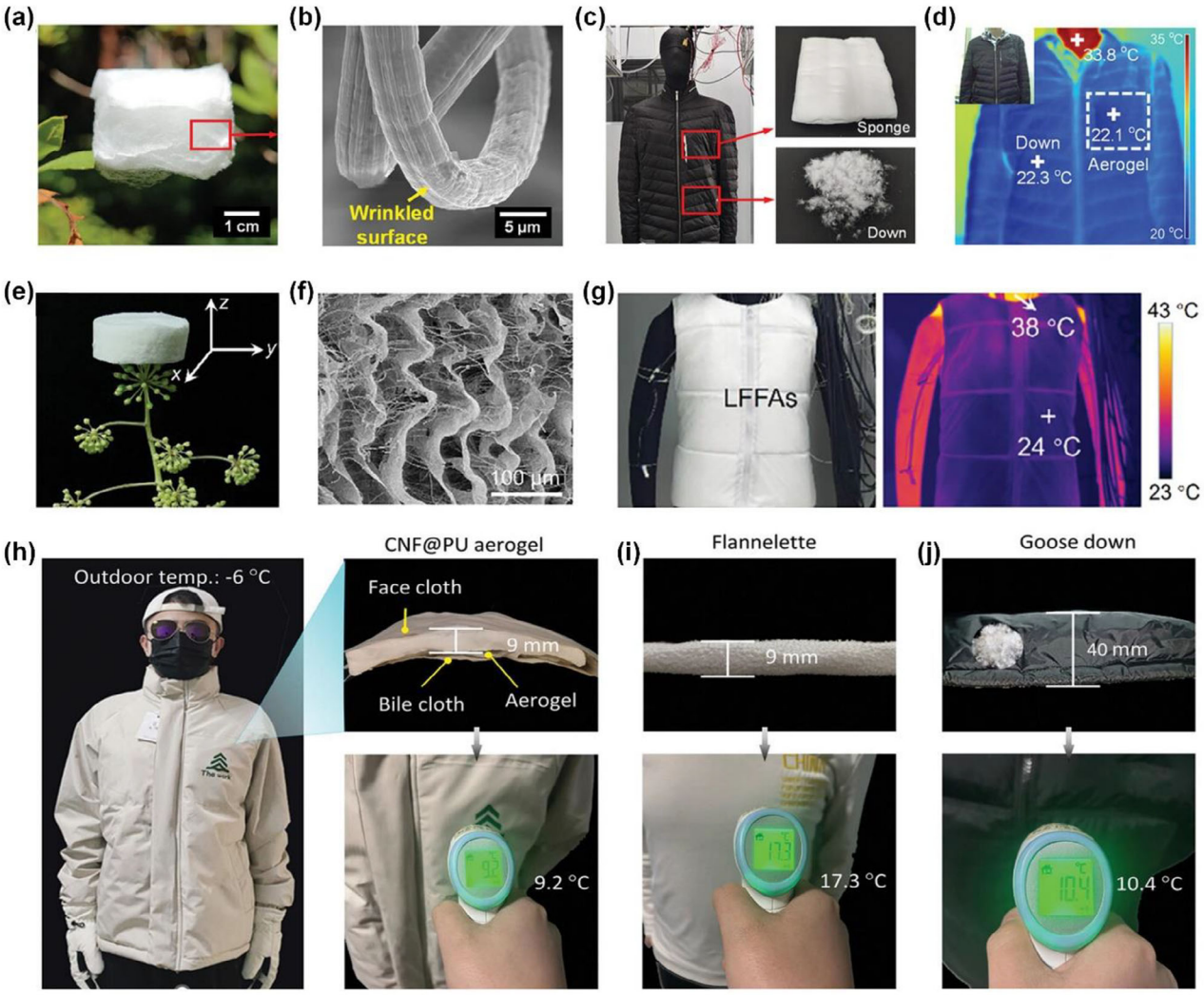

Figure 12. a) An optical image illustrating the ultralight property of sponges. b) SEM image of the curly wrinkled fibers. c) Optical image of thermal mannequins test. d) Comparing the thermal insulation performance of the aerogel and commercial down feather. e) Photograph showing the ultralight standing on the flower. f) SEM image of the 3D aerogels. g) Photographs and IR images of thermal manikin covered by the 3D aerogel clothing. h) Measured the thermal insulation performance of the home-made aerogel cloth in −6 °C. Monitoring the surface temperature of i) self-made jacket and j) goose down. Reproduced with permission.[137] Copyright 2023, Wiley-VCH. Reproduced with permission.[140] Copyright 2024, Wiley-VCH. Reproduced with permission.[110] Copyright 2024, Wiley-VCH.

During high-speed flight, significant friction arises between the spacecraft surface and the surrounding air, leading to extreme aerodynamic heat generation. Therefore, a thermal protection system must be integrated into their surfaces to effectively manage the cumulative heat load. Moreover, a lightweight heat shield is crucial for facilitating vehicles to undertake long-distance flights. The micro/nanofiber thermal insulation ceramic aerogels possess high porosity (>80%) and high-temperature resistance, becoming the potential candidate for heat insulators applied in the aerospace industry.[50] To develop a high-performance thermal protection system, researchers have carried out a great deal of work, mainly focusing on improving thermal insulation properties, thermal resistance range, and mechanical properties. For example, Zhang *et al*, inspired by the durable protective shells of mollusks, developed multi-mechanical synergistic ceramic aerogels by constructing 3D architecture through the precise assembly of nanofibers and nanosheets (**Figure 13a**).[141] By engineering a hierarchical multi-arched structure to dissipate stress, the aerogel exhibited outstanding compressive resilience, bendability, and mechanical robustness. Moreover, the aerogels showed remarkable thermal resilience, maintaining structural integrity from cryogenic (−196 °C) to ultrahigh temperatures (1100 °C), while achieving superior insulation performance (39.72 mW m^{-1} K^{-1}). Interestingly, the surface temperature of the biomimetic ceramic aerogels put on the metal model aircraft of 400 °C maintains an internal room temperature, indicating their potential to shield onboard instruments in high-speed aircraft (Figure 13b,c). Similarly, Wang and co-workers fabricated the biomimetic bouligand-chiral ceramic aerogels (BcF-CAs) based on the layer-by-layer stacking method.[46] The

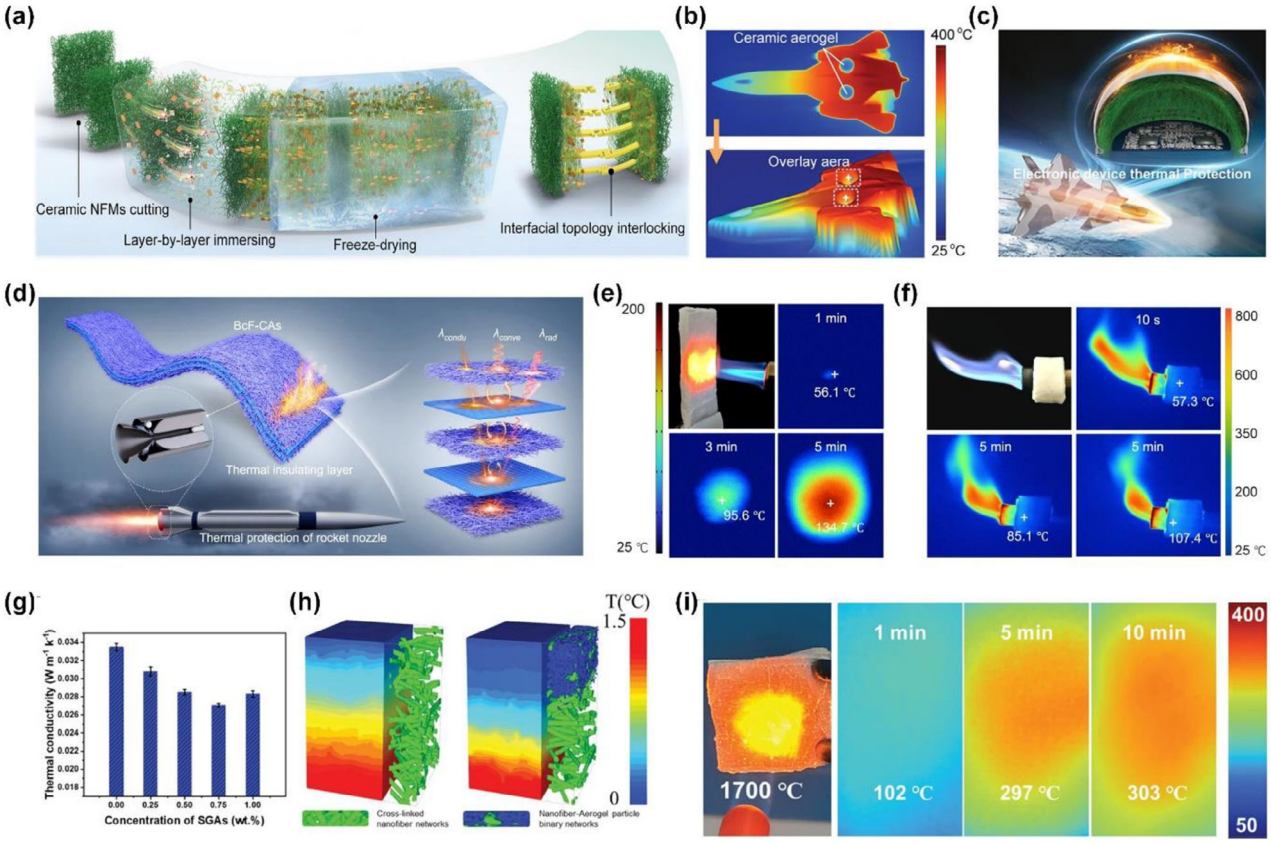

Figure 13. a) Schematic diagram of fabricating biomimetic ceramic aerogels. b) IR images showing the surface temperature of an aircraft model covered by the aerogel. c) Presented as a thermal barrier for aerospace electronics. d) The heat transfer mechanism in the BcF-CAs. Optical and IR images of the BcF-CAs e) exposed to the butane blow torch and f) protected butane nozzle. g) Thermal conductivity of ceramic meta-aerogel. h) Simulating the thermal insulation property of the meta-aerogel materials. i) Optical and IR images of the meta-aerogel at 1700 °C. Reproduced with permission.[141] Copyright 2024, Wiley-VCH. Reproduced with permission.[46] Copyright 2024, Springer Nature. Reproduced with permission.[142] Copyright 2024, Wiley-VCH.

resulting aerogels demonstrated exceptional mechanical performance at high temperatures and remarkable thermal stability (>1200 °C), making them highly attractive candidates for thermal barriers in the aerospace industry (Figure 13d–f). However, under extremely high-temperature conditions (>1500 °C), uncontrolled grain growth could lead to irreversible structural damage in ceramic aerogels, significantly accelerating degradation and greatly raising the risk of catastrophic failures. To solve the bottleneck problem, Xu et al. designed the ceramic meta-aerogel with ultralow thermal conductivity of 27 mW m^{-1} K^{-1} and thermomechanical stability under extreme conditions (Figure 13g).[142] Significantly, the aerogels maintain structural stability at 1700 °C attributed to the phase transition modulation of Al_2O_3 by amorphous SiO_2 (Figure 13h,i). The exceptional thermal insulation properties of the meta aerogel make it highly suitable for safeguarding aerospace equipment under extreme high-temperature conditions.

In summary, micro/nanofiber thermal insulation materials have demonstrated remarkable potential in aerospace applications attributed to their lightweight characteristic, excellent thermal resistance, and adaptability to extreme environments. These materials not only enhance the thermal protection of aerospace equipment but also contribute to energy efficiency and structural optimization. As research continues to advance, further innovations in micro/nanofiber structure and fabrication techniques are expected to unlock even greater performance, solidifying their role as a critical component in the future of aerospace engineering.

5.3. Automobile Industry

The rapid development of the automobile industry, including electric vehicles and hybrid electric vehicles, has brought about new challenges and opportunities in thermal management.[143] Lithium-ion batteries, as the core power source of new energy vehicles, have revolutionized the automotive industry with their high energy density and long cycle life.[144] However, their inherent flammability poses significant safety challenges. Under abusive conditions such as overcharging, mechanical damage, or thermal exposure, lithium-ion batteries are prone to thermal runaway, a chain reaction leading to rapid temperature rise, gas release, and even fire or explosion. Once thermal runaway occurs in a single cell, the generated heat can propagate to adjacent cells, resulting in catastrophic failure of the entire battery pack.[145,146] To address this critical safety issue, effective thermal insulation

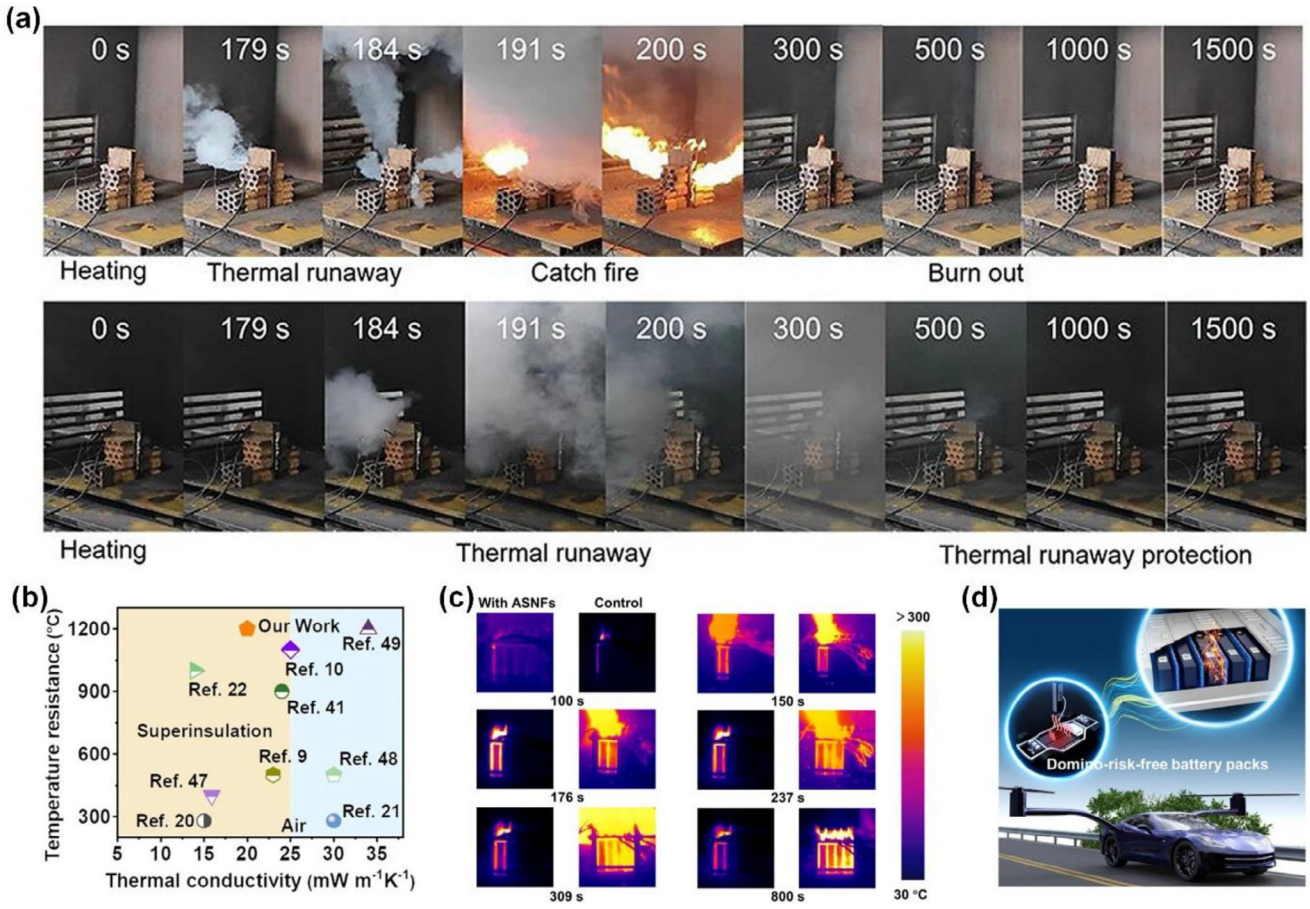

Figure 14. a) Schematic diagram of the aerogels applied in flying EV. b) Comparing the thermal conductivity and temperature resistance of various ultralight materials. c) Time-dependent images were taken during TR propagation testing caused by overheat. d) Observe the thermal runaway processes. Reproduced with permission.[147] Copyright 2024, American Chemical Society. Reproduced with permission.[113] Copyright 2023, Springer Nature.

materials are urgently needed to prevent or delay heat propagation, providing valuable time for emergency response and minimizing potential damage.

Benefiting from the 3D interconnected porous network structure that can trap gas molecules and minimize heat transfer, the micro/nanofiber ceramic aerogels or sponges exhibit remarkable thermal insulation and temperature endurance properties. Researchers have demonstrated the outstanding capability of ceramic aerogels in suppressing thermal runaway propagation within battery systems. Additionally, their lightweight characteristics ensure minimal reduction in the overall energy density of battery packs, making them an ideal candidate for enhancing thermal management in energy storage applications. For example, Feng et al. developed ceramic sponge consisting of microfiber and nanofiber networks via direct electrospinning techniques.[147] The resulting micro/nanofiber sponge showed a low volume density of 6.21 mg cm^{-3}, a small thermal conductivity of 22 mW m^{-1} K^{-1}, and high temperature resistance of ≈1300 °C. As shown in **Figure** 14a, compared with the air control group, the battery packs burned quickly, caused by a vicious cycle of heat accumulation, and no combustion occurred in the battery packs protected by the ceramic sponges. Similarly, Li and co-workers constructed the Al_2O_3·SiO_2 nanofiber aerogels with low thermal conductivity of 25 mW m^{-1} K^{-1} via freeze-drying method (Figure 14b).[113] Because of the robust thermal insulation and heat stability, ceramic sponges were successfully applied in the automobile industry. As presented in Figure 14c, the ceramic aerogels demonstrated an impressive heat-shielding performance with an impressive temperature differential of 315 °C, effectively preventing the surface temperature of the adjacent battery from reaching the critical thermal runaway threshold of ≈200 °C. Such significant thermal barrier highlights their exceptional capability in mitigating heat propagation and enhancing battery safety (Figure 14d).

5.4. Other Applications

Beyond well-documented applications in personal thermal protection, aerospace, and new energy vehicles, micro/nanofiber thermal insulation materials have demonstrated remarkable versatility in a variety of other fields.[148–152] Their unique properties, such as low thermal conductivity, lightweight design, and heat resistance, make them suitable for addressing diverse challenges across industries. For instance, their exceptional noise absorption capabilities have opened new possibilities for

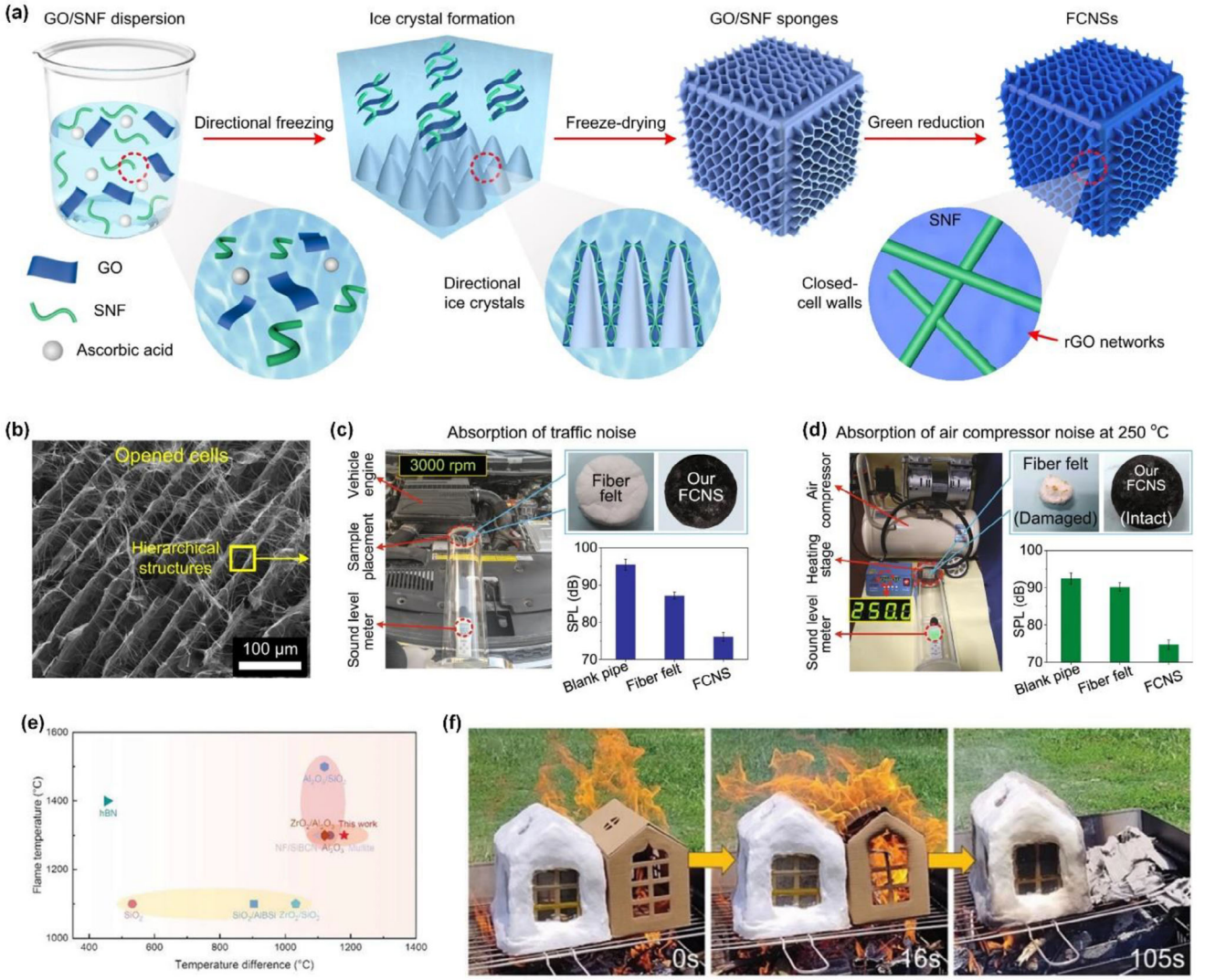

Figure 15. a) Schematic illustration of the preparation of FCNSs. b) The microscopic structure of FCNSs. c) Aerogels applied in automobile engine noise absorption. d) The noise absorption of the aerogels. e) Comparing the flame resistance of various aerogels. f) The heat-insulating and fire-retardant demonstration of the hybrid ceramic aerogel. Reproduced with permission.[154] Copyright 2021, Springer Nature. Reproduced with permission.[156] Copyright 2023, Wiley-VCH.

reducing acoustic pollution, while their thermal insulation performance has been leveraged to enhance energy efficiency in buildings. This section explores the expanding applications of micro/nanofiber thermal insulation materials, such as noise reduction and building energy management.

As the traffic industry advances rapidly, noise pollution from traffic has emerged as a growing threat to the global economy, ecological balance, and public health, acting as an invisible yet significant hazard.[153] Therefore, utilizing the fibrous porous materials to mitigate traffic noise is crucial for addressing and minimizing unwanted sound. Nevertheless, the conventional microfibrous noise-absorbing materials exhibited poor absorption of noise originating from the inherent defects of large fiber diameter and low porosity. Additionally, polymer-based fibrous noise-absorbing materials face the problem of structural instability at high temperatures because of the low decomposition temperature (usually <150 °C). Fortunately, the 3D micro/nanofiber ceramic aerogels could provide the solution for controlling traffic noise. Zong et al. fabricated flexible ceramic nanofibrous aerogels (FCNSs) with a hierarchical network structure based on the freeze-drying method (**Figure 15**a,b).[154] The resulting ceramic sponges exhibited a lightweight feature of 9.3 mg cm^{-3} and excellent temperature-invariant stability from −100 to 500 °C. Meaningfully, the sponges could effectively absorb the automobile engines noise, as shown in Figure 15c. Compared with the fiber felt with 8.3 dB noise attenuation, the nanofiber ceramic sponges could reduce noise by 19.4 dB. Moreover, the sponges also achieved 17.7 dB noise attenuation at the high temperature of 250 °C, whereas the polymer felt was completely ineffective (Figure 15d). These findings demonstrate that the thermal insulation ceramic aerogels could serve as highly effective noise-absorbing materials,

offering promising potential for reducing traffic-related noise pollution.

The building industry faces increasing challenges related to fire safety, particularly as modern buildings demand higher performance in thermal insulation and fire resistance.[155] Traditional insulation materials often fall short of meeting these requirements, especially under extreme conditions such as high temperatures or direct exposure to flames. The micro/nanofiber ceramic thermal insulation materials have emerged as a promising solution to address these critical issues. For example, Cheng et al. developed the SiO_2/Al_2O_3 hybrid ceramic aerogel with low thermal conductivity (29 mW m^{-1} K^{-1}) and high-temperature reduction (1179.6 °C) based on the freeze-drying method (Figure 15e).[156] As shown in Figure 15f, when exposed to a fire, the paper house was burned to ashes in 105 s, while the house protected by the ceramic sponges remained intact and unburned. This result demonstrates that the micro/nanofiber ceramic materials possess high-efficiency fire resistance, holding significant potential and engineering significance in high-temperature protection for buildings.

6. Conclusions and Perspectives

Thermal insulation materials are indispensable in both everyday life and industrial applications, providing efficient insulation solutions that minimize energy consumption, improve personal comfort, and drive advancements in the aerospace industry. Compared with conventional natural and synthetic fiber materials, micro/nanofiber thermal insulation materials have emerged as a promising solution for diverse applications due to their unique structural advantage, including small fiber diameter, tunable porosity, and lightweight. Significant advancements have been achieved in the research of micro/nanofiber thermal insulation materials attributed to persistent efforts and continuous exploration. Up to now, various forms of the micro/nanofiber thermal insulation materials, mainly involving the 2D micro/nanofibrous membranes/textiles and 3D bulk materials, have been developed based on a variety of methods, like freeze-drying method, direct electrospinning, layer-by-layer stacking, and solution blow spinning. Benefiting from the enhanced structural integrity and superior thermal insulation performance, the micro/nanofiber thermal insulation materials have potential applications ranging from personal thermal management to high-performance insulation in aerospace, traffic, and building industries. Consequently, we present a comprehensive analysis of recent advancements and investigations spanning from heat transfer mechanisms to fabrication techniques to the multifunctional applications of micro/nanofiber-based porous thermal insulation materials.

Despite significant advancements in micro/nanofiber thermal insulation materials, critical challenges and unresolved issues remain to be tackled through substantial research endeavors in the coming years. Herein, we put forward some insights aimed at offering valuable guidance to enhance the performance and expand the future potential of the micro/nanofiber porous thermal insulation materials.

1) Exploration of thermal insulation mechanism. Early investigations primarily focused on optimizing the composition, porous structure, and morphology design of micro/nanofiber porous materials to enhance the thermal insulation properties. However, there has been insufficient exploration into thermal diffusion behaviors in micro/nanofiber porous materials. Therefore, the correlation between structural characteristics (such as fiber diameter, surface roughness, pore size, and pore tortuosity) and thermal insulation performance needs to be established based on model analysis and finite element simulation. Study of dynamic thermal transfer and dissipation processes within the micro/nanofiber porous materials under external force will offer foundational insights for enhancing the dynamic thermal insulation performance.
2) Structural stability and durability. The long-term structural integrity of micro/nanofiber porous materials under various environmental conditions poses a significant challenge, particularly for 3D porous structures. To address the problem, future research can focus on single-fiber mechanical reinforcement and fiber assembly mechanical reinforcement. For single fibers, high-strength polymers or composite materials, such as carbon nanotubes or graphene, can be used to enhance mechanical properties. Simultaneously, the fiber assembly can be reinforced through inter-fiber bonding, hierarchical structure design, and controlled porosity to ensure even load distribution and structural cohesion.
3) Large-scale and green production. The sustainable development of high-performance micro/nanofiber thermal insulation materials also faces a huge challenge. Although the above-mentioned methods, such as the freeze-drying method, direct electrospinning, and layer-by-layer stacking, could manufacture various types of efficient micro/nanofiber thermal insulation materials, these techniques present a low production rate and are far from achieving industrialization; moreover, the majority of micro/nanofiber thermal insulation materials are fabricated by utilizing organic solvents like *N*,*N*-dimethylformamide, *N*,*N*-dimethylacetamide, and tetrahydrofuran, leading to significant health hazard and environmental pollution. Therefore, innovative and scalable methods to produce environmentally friendly and high-performance micro/nanofiber thermal insulation materials are highly desirable, particularly through a low-carbon emission biomimicry approach.
4) Multifunctionality and intelligence. The development of micro/nanofiber-based thermal insulation materials should pivot toward multifunctional integration to address evolving industrial and environmental needs. Future thermal insulation materials should not only possess efficient thermal insulation properties but also integrate other functions, such as antibacterial, fire-resistant, and self-cleaning capabilities. With the development of smart materials, the next-generation fiber-based insulators will be able to automatically regulate heat conduction based on environmental temperature and human needs.

Despite existing numerous challenges, we are confident that ongoing research and development in micro/nanofiber thermal insulation materials will overcome existing limitations and drive their widespread application in healthcare, energy, and environmental fields.

Acknowledgements

The work described in this paper was partly supported by a grant from the Research Grants Council of the Hong Kong Special Administrative Region, China (Project No. PolyU 15209623). Support from the RGC Postdoctoral Fellowship Scheme (P0052633) is also acknowledged.

Conflict of Interest

The authors declare no conflict of interest.

Keywords

2D fibrous membranes and textiles, 3D sponges/aerogels, micro/nanofiber, pore structures, thermal insulation

Received: April 15, 2025
Revised: June 25, 2025
Published online: September 25, 2025

[1] Z. Jiang, S. Karan, A. G. Livingston, *Adv. Mater.* **2018**, *30*, 1705973.
[2] P. Wollburg, S. Hallegatte, D. G. Mahler, *Nature* **2023**, *623*, 982.
[3] F. Vidal, E. Marel, R. F. Kerr, C. McElroy, N. Schroeder, C. Mitchell, G. Rosetto, T. Chen, R. M. Bailey, C. Hepburn, C. Redgwell, C. K. Williams, *Nature* **2023**, *626*, 7997.
[4] P. Hsu, A. Y. Song, P. B. Catrysse, C. Liu, Y. Peng, J. Xie, S. Fan, Y. Cui, *Science* **2016**, *353*, 6303.
[5] Y. Ding, C. H. Dreimol, R. Zboray, K. Tu, S. Stucki, T. Keplinger, G. Panzarasa, I. Burgert, *Mater. Horiz.* **2023**, *10*, 257.
[6] C. Guo, H. Tang, P. Wang, Q. Xu, H. Pan, X. Zhao, F. Fan, T. Li, D. Zhao, *Nat. Commun.* **2024**, *15*, 6100.
[7] M. Li, W. Zhang, Y. Geng, B. Lu, J. He, J. Liu, X. Li, H. Zhou, X. Fan, J. Zhai, *Adv. Funct. Mater.* **2025**, *35*, 2414342.
[8] N. L. Panwar, S. C. Kaushik, S. Kothari, *Renewable Sustainable Energy Rev.* **2011**, *15*, 1513.
[9] F. Xiong, J. Zhou, Y. Jin, Z. Zhang, M. Qin, H. Han, Z. Shen, S. Han, X. Geng, K. Jia, R. Zou, *Nat. Commun.* **2024**, *15*, 7125.
[10] Q. Zhang, H. Huang, C. Lei, Y. Liu, W. Li, *Materials* **2025**, *18*, 2383.
[11] J. Feng, Z. Ma, J. Wu, Z. Zhou, Z. Liu, B. Hou, W. Zheng, S. Huo, Y. T. Pan, M. Hong, Q. Gao, Z. Sun, H. Wang, P. Song, *Adv. Mater.* **2025**, *37*, 2411856.
[12] B. Wu, Q. Qi, L. Liu, Y. Liu, J. Wang, *ACS Nano* **2024**, *18*, 9798.
[13] X. Liu, W. Zhu, P. Deng, T. Li, *ACS Nano* **2023**, *17*, 18657.
[14] Z. Yu, N. Yang, L. Zhou, Z. Ma, Y. Zhu, Y. Lu, B. Qin, W. Xing, T. Ma, S. Li, H. Gao, H. Wu, S. Yu, *Sci. Adv.* **2018**, *4*, aat7223.
[15] B. Gu, Q. Xu, H. Wang, H. Pan, D. Zhao, *ACS Nano* **2023**, *17*, 18308.
[16] X. Leng, L. Liu, S. Liu, Y. Li, Y. Xiao, L. Bao, M. Zhu, Q. Zhou, T. Zhu, L. Xue, Z. Liu, X. Zhou, *Adv. Funct. Mater.* **2025**, *35*, 2416912.
[17] J. Zhu, Y. Zhu, Y. Ye, Z. Qiu, Y. Zhang, Z. Yu, X. Sun, D. C. Bressler, F. Jiang, *Adv. Funct. Mater.* **2023**, *33*, 2300893.
[18] S. Wang, C. Liu, F. Wang, X. Yin, J. Yu, S. Zhang, B. Ding, *Adv. Fiber Mater.* **2023**, *5*, 847.
[19] H. Zhong, Y. Li, P. Zhang, S. Gao, B. Liu, Y. Wang, T. Meng, Y. Zhou, H. Hou, C. Xue, Y. Zhao, Z. Wang, *ACS Nano* **2021**, *15*, 10076.
[20] Z. Y. Wang, Z. C. Li, B. Li, A. F. Shi, L. Zhang, Y. B. Zhu, F. Ye, S. H. Yu, *Adv. Mater.* **2024**, *36*, 2412605.
[21] L. Su, H. Wang, S. Jia, S. Dai, M. Niu, J. Ren, X. Lu, Z. Cai, D. Lu, M. Li, L. Xu, S. W. Guo, L. Zhuang, K. Peng, H. Stretchable, *ACS Nano* **2021**, *15*, 18354.
[22] H. Xu, S. Wang, X. Gong, M. Yang, X. Liu, S. Zhang, J. Yu, B. Ding, *Compos. Commun.* **2022**, *29*, 101024.
[23] S. Zhang, H. Liu, N. Tang, J. Ge, J. Yu, B. Ding, *Nat. Commun.* **2019**, *10*, 1458.
[24] S. Chen, Y. Chen, Y. Zhao, L. Zhang, C. Zhu, Y. Zhang, S. Liu, S. Xia, J. Yu, B. Ding, J. Yan, *Mater. Today* **2022**, *61*, 139.
[25] X. Long, J. Qin, J. Tang, J. Xue, Y. Wang, L. Zhou, S. Wang, X. Wei, Y. Lin, J. Liao, *Adv. Funct. Mater.* **2024**, *35*, 2413018.
[26] Y. Cheng, H. Cheng, J. Gao, Y. Xue, G. Han, B. Zhou, C. Liu, Y. Feng, C. Shen, *Small* **2025**, *21*, 2409408.
[27] K. M. Chung, S. R. Adapa, Y. Pei, R. H. Yeerella, L. Chen, S. Shivakumar, W. Huang, Z. Liu, S. Cai, J. Luo, R. Chen, *Adv. Mater.* **2025**, *37*, 2406732.
[28] P. C. Hsu, X. Liu, C. Liu, X. Xie, H. R. Lee, A. J. Welch, T. Zhao, Y. Cui, *Nano Lett.* **2015**, *15*, 365.
[29] Y. Si, X. Wang, C. Yan, L. Yang, J. Yu, B. Ding, *Adv. Mater.* **2016**, *28*, 9512.
[30] L. Cai, A. Y. Song, P. Wu, P. C. Hsu, Y. Peng, J. Chen, C. Liu, P. B. Catrysse, Y. Liu, A. Yang, C. Zhou, C. Zhou, S. Fan, Y. Cui, *Nat. Commun.* **2017**, *8*, 496.
[31] Y. Cui, H. Gong, Y. Wang, D. Li, H. Bai, *Adv. Mater.* **2018**, *30*, 1706807.
[32] Z. Liu, J. Lyu, D. Fang, X. Zhang, *ACS Nano* **2019**, *13*, 5703.
[33] C. Jia, L. Li, Y. Liu, B. Fang, H. Ding, J. Song, Y. Liu, K. Xiang, S. Lin, Z. Li, W. Si, B. Li, X. Sheng, D. Wang, X. Wei, H. Wu, *Nat. Commun.* **2020**, *11*, 3732.
[34] W. Sakuma, S. Yamasaki, S. Fujisawa, T. Kodama, J. Shiomi, K. Kanamori, T. Saito, M. Strong, *ACS Nano* **2021**, *15*, 1436.
[35] X. Cheng, Y. T. Liu, Y. Si, J. Yu, B. Ding, *Nat. Commun.* **2022**, *13*, 2637.
[36] Y. Tian, S. Wang, M. Yang, S. Liu, J. Yu, S. Zhang, B. Ding, *ACS Nano* **2023**, *17*, 25439.
[37] X. Chang, F. Wu, X. Cheng, H. Zhang, L. He, W. Li, X. Yin, J. Yu, Y. T. Liu, B. Ding, *Adv. Mater.* **2024**, *36*, 2308519.
[38] W. Wang, Q. Fu, J. Ge, S. Xu, Q. Liu, J. Zhang, *Molecules* **2024**, *29*, 2279.
[39] C. Liu, Y. Liao, W. Jiao, X. Zhang, N. Wang, J. Yu, Y. T. Liu, B. Ding, *Adv. Mater.* **2023**, *35*, 2304401.
[40] Y. Tian, Y. Chen, S. Wang, X. Wang, J. Yu, S. Zhang, B. Ding, *Nat. Commun.* **2024**, *15*, 6416.
[41] Y. Fu, H. Wang, C. Zhou, Y. Wang, N. Li, *Polymer* **2024**, *297*, 126822.
[42] P. Hu, F. Wu, B. Ma, J. Luo, P. Zhang, Z. Tian, J. Wang, Z. Sun, *Adv. Mater.* **2024**, *36*, 2310023.
[43] C. Li, Y. Duan, S. Wang, S. Wang, D. Yu, L. Wang, Y. Wang, M. Wu, *ACS Appl. Mater. Interfaces* **2024**, *16*, 14124.
[44] T. Xue, C. Zhu, D. Yu, X. Zhang, F. Lai, L. Zhang, C. Zhang, W. Fan, T. Liu, *Nat. Commun.* **2023**, *14*, 8378.
[45] H. Wu, L. Zhao, S. Zhang, Y. Si, J. Yu, B. Ding, *ACS Appl. Mater. Interfaces* **2021**, *13*, 18165.
[46] H. Wang, L. Cheng, J. Yu, Y. Si, B. Ding, *Nat. Commun.* **2024**, *15*, 336.
[47] Y. Si, X. Wang, L. Dou, J. Yu, B. Ding, *Sci. Adv.* **2018**, *4*, aas8925.
[48] H. Liu, X. Huo, P. Zhao, R. Xu, X. Zhang, J. Yu, Y. T. Liu, B. Ding, *ACS Nano* **2024**, *18*, 29273.
[49] R. Zhang, X. Gong, S. Wang, Y. Tian, Y. Liu, S. Zhang, J. Yu, B. Ding, *ACS Appl. Mater. Interfaces* **2021**, *13*, 58027.
[50] L. Dou, X. Zhang, H. Shan, X. Cheng, Y. Si, J. Yu, B. Ding, *Adv. Funct. Mater.* **2020**, *30*, 2005928.
[51] S. Wang, R. Ding, G. Liang, W. Zhang, F. Yang, Y. Tian, J. Yu, S. Zhang, B. Ding, *Adv. Mater.* **2024**, *36*, 2313444.
[52] K. Uetani, K. Hatori, *Sci. Technol. Adv. Mater.* **2017**, *18*, 877.
[53] W. Wu, X. Wang, X. Han, Z. Yang, G. Gao, Y. Zhang, J. Hu, Y. Tan, A. Pan, C. Pan, *Adv. Mater.* **2019**, *31*, 1805913.
[54] V. Kalkavoura, P. Munier, L. Bergstrom, *Adv. Mater.* **2021**, *33*, 2001839.
[55] Z. Niu, F. Qu, F. Chen, X. Ma, B. Chen, L. Wang, M. Xu, S. Wang, L. Jin, C. Zhang, X. Hou, *Nano-Micro Lett.* **2024**, *16*, 200.
[56] J. F. Guo, G. H. Tang, *Int. J. Heat Mass Transfer* **2019**, *137*, 64.

[57] M. Dehbani, M. Rahimi, Z. Rahimi, *Appl. Therm. Eng.* **2022**, *208*, 118273.
[58] S. Zhang, S. Meng, K. Zhang, Z. Wang, X. Xu, C. Zhi, S. Shi, J. Hu, *Nano Energy* **2023**, *112*, 108443.
[59] J. Chai, J. Fan, *Adv. Energy Mater.* **2022**, *13*, 2202932.
[60] W. Yu, C. Liu, S. Fan, *Nano Res.* **2021**, *14*, 2471.
[61] X. Chang, X. Cheng, H. Zhang, W. Li, L. He, X. Yin, X. Liu, J. Yu, Y. T. Liu, B. Ding, *Adv. Funct. Mater.* **2023**, *33*, 2215168.
[62] B. Wang, L. Li, F. Schäfer, J. J. Pottas, A. Kumar, V. M. Wheeler, W. Lipiński, *Chem. Eng. J.* **2021**, *412*, 128255.
[63] X. Xu, J. Chen, J. Zhou, B. Li, *Adv. Mater.* **2018**, *30*, 1705544.
[64] Flores, R. K. B, D. Nestler, W. Krenkel, G. Motz, *Adv. Eng. Mater.* **2014**, *16*, 621.
[65] X. Zhang, J. Yu, C. Zhao, Y. Si, *Small* **2024**, *20*, 2311464.
[66] X. Gong, M. Ding, P. Gao, X. Liu, J. Yu, S. Zhang, B. Ding, *Adv. Mater.* **2023**, *35*, 2305606.
[67] H. Lin, Q. Shen, M. Ma, R. Ji, H. Guo, H. Qi, W. Xing, H. Tang, *Adv. Sci.* **2025**, *12*, 2412554.
[68] Y. Yang, Z. Chen, T. Vogt Wu, A. Sempey, J. Batsale, *Int. J. Therm. Sci* **2022**, *181*, 107687.
[69] Z. Liu, Z. Sheng, Y. Bao, Q. Cheng, P. X. Wang, Z. Liu, X. Zhang, *ACS Nano* **2023**, *17*, 18411.
[70] C. Bi, G. H. Tang, Z. J. Hu, H. L. Yang, J. N. Li, *Int. J. Heat Mass Transfer* **2014**, *79*, 126.
[71] Y. Lee, J. Moon, D. Choi, M. Ko, *Sustainability* **2024**, *16*, 5687.
[72] H. Zhang, C. Shang, G. Tang, *Int. J. Therm. Sci* **2022**, *171*, 107261.
[73] B. Abad, D. Tasciuc, M. Gonzalez, *Renewable Sustainable Energy Rev.* **2017**, *76*, 1348.
[74] C. Sun, J. Luo, S. Yan, K. Li, Y. Li, H. Wang, C. Hou, Q. Zhang, *Adv. Funct. Mater.* **2022**, *33*, 2211035.
[75] B. Yuan, B. Yang, P. Xu, M. Zhang, *ACS Nano* **2025**, *19*, 1981.
[76] J. Kocsis, H. Mahmood, A. Pegoretti, *Prog. Mater. Sci.* **2015**, *73*, 1.
[77] J. Chang, L. Shi, M. Zhang, R. Li, Y. Shi, X. Yu, K. Pang, L. Qu, P. Wang, J. Yuan, *Adv. Mater.* **2023**, *35*, 2209215.
[78] M. Lian, W. Ding, S. Liu, Y. Wang, T. Zhu, Y. E. Miao, C. Zhang, T. Liu, *Nano-Micro Lett.* **2024**, *16*, 131.
[79] F. L. Zhu, Q. Q. Feng, *Int. J. Therm. Sci.* **2021**, *165*, 106899.
[80] Q. Gao, T. Lauster, B. A. F. Kopera, M. Retsch, S. Agarwal, A. Greiner, *Adv. Funct. Mater.* **2021**, *32*, 2108808.
[81] C. Yuan, D. Zhang, Y. Gan, *ACS Omega* **2024**, *9*, 28912.
[82] P. Qiu, R. Jin, Y. Son, A. Ju, W. Jiang, L. Wang, W. Luo, *Adv. Fiber Mater.* **2024**, *6*, 658.
[83] X. Chen, M. Sun, L. Cao, H. Rong, H. Lin, Y. Chen, M. Zhang, L. Zhang, B. Xiao, W. Li, J. Fang, L. Sun, S. Zhang, S. Y. Tang, X. Li, *Adv. Mater.* **2024**, *36*, 2404705.
[84] B. Zhao, J. Huang, Q. Wang, H. Huang, Q. Chen, *Ceram. Int.* **2023**, *49*, 35722.
[85] D. Ma, Y. Xie, L. Wang, Y. Peng, Y. Yin, X. Wang, B. Liu, G. Zhang, L. Zhu, D. Xu, *Chem. Eng. J.* **2023**, *468*, 143488.
[86] B. Zhao, H. Huang, Q. Chen, *J. Non-Cryst. Solids* **2022**, *594*, 121809.
[87] Q. Cheng, Z. Sheng, Y. Ding, Y. Li, X. Zhang, *Prog. Mater. Sci.* **2025**, *152*, 101456.
[88] C. Shao, H. Kim, J. Gong, D. Lee, *Nanotechnology* **2002**, *13*, 635.
[89] Y. Si, X. Mao, H. Zheng, J. Yu, B. Ding, *RSC Adv.* **2015**, *5*, 6027.
[90] Z. Zhang, C. Liu, N. Li, W. Guo, Y. Li, P. Yang, S. Zhang, Z. Wang, *Adv. Sci.* **2025**, *12*, 2416740.
[91] X. Mao, J. Hong, Y. X. Wu, Q. Zhang, J. Liu, L. Zhao, H. H. Li, Y. Y. Wang, K. Zhang, *Nano Lett.* **2021**, *21*, 9419.
[92] N. Wang, Y. Xie, J. Lv, J. Zhang, L. Zhu, Z. Jia, X. Tao, *Ceram. Int.* **2022**, *48*, 19460.
[93] S. Li, X. Cheng, G. Han, Y. Si, Y. Liu, J. Yu, B. Ding, *J. Colloid Interface Sci.* **2023**, *636*, 83.
[94] Y. Liu, H. Wang, J. Hao, Y. Cheng, S. Dong, P. Hu, W. Han, X. Zhang, *Extreme Mater.* **2025**, *1*, 38.
[95] Z. Xu, H. Liu, F. Wu, L. Cheng, J. Yu, Y. T. Liu, B. Ding, *Adv. Mater.* **2023**, *35*, 2305336.
[96] H. Guo, J. Sun, J. Ge, D. Han, Y. Lv, P. Hu, C. Wang, Y. Liu, *Ceram. Int.* **2024**, *50*, 4936.
[97] M. Li, F. Gan, J. Dong, Y. Fang, X. Zhao, Q. Zhang, *ACS Appl. Mater. Interfaces* **2021**, *13*, 10416.
[98] X. Song, H. Gong, H. Li, M. Zhang, L. Jiang, C. Wang, P. Jiang, H. Wang, K. Cao, G. Liu, Q. Zhao, T. Fan, *Adv. Funct. Mater.* **2024**, *35*, 2413191.
[99] Y. Wang, Y. Cui, Z. Shao, W. Gao, W. Fan, T. Liu, H. Bai, *Chem. Eng. J.* **2020**, *390*, 124623.
[100] T. Xue, C. Zhu, X. Feng, Q. Wali, W. Fan, T. Liu, *Adv. Fiber Mater.* **2022**, *4*, 1118.
[101] T. Xue, Y. Yu, Z. Fu, Q. Wang, Z. Hu, W. Fan, T. Liu, *Compos. Sci. Technol.* **2023**, *242*, 110196.
[102] C. Zhu, T. Xue, Z. Ma, W. Fan, T. Liu, *ACS Appl. Mater. Interfaces* **2023**, *15*, 12443.
[103] Tafreshi, Z. S, S. Mosanenzadeh, M. M. Rastegardoost, C. Zhang, C. B. Park, H. E. Naguib, *ACS Appl. Mater. Interfaces* **2024**, *16*, 54597.
[104] M. Wu, Z. Shao, N. Zhao, R. Zhang, G. Yuan, L. Tian, Z. Zhang, W. Gao, H. Bai, *Science* **2023**, *382*, 1379.
[105] Z. Liu, J. Lyu, Y. Ding, Y. Bao, Z. Sheng, N. Shi, X. Zhang, *ACS Nano* **2022**, *16*, 15237.
[106] J. Wang, D. Liu, Q. Li, C. Chen, Z. Chen, P. Song, J. Hao, Y. Li, S. Fakhrhoseini, M. Naebe, X. Wang, W. Lei, *ACS Nano* **2019**, *13*, 7860.
[107] H. Liu, X. Chen, Y. Zheng, D. Zhang, Y. Zhao, C. Wang, C. Pan, C. Liu, C. Shen, *Adv. Funct. Mater.* **2021**, *31*, 2008006.
[108] Y. Si, J. Yu, X. Tang, J. Ge, B. Ding, *Nat. Commun.* **2014**, *5*, 5802.
[109] H. Wu, H. Cai, S. Zhang, J. Yu, B. Ding, *Nano Lett.* **2022**, *22*, 830.
[110] G. Wang, J. Feng, Z. Zhou, Z. Liu, J. Wu, J. Li, Q. Gao, M. Lynch, J. Li, P. Song, *Adv. Mater.* **2024**, *37*, 2414896.
[111] J. Wu, J. Zhang, M. Sang, Z. Li, J. Zhou, Y. Wang, S. Xuan, K. C. F. Leung, X. Gong, *Adv. Funct. Mater.* **2023**, *34*, 2307072.
[112] Di, C. S, S. E. Hadi, L. Bergstrom, *Adv. Mater.* **2023**, *35*, 2305195.
[113] L. Li, Y. Zhou, Y. Gao, X. Feng, F. Zhang, W. Li, B. Zhu, Z. Tian, P. Fan, M. Zhong, H. Niu, S. Zhao, X. Wei, J. Zhu, H. Wu, *Nat. Commun.* **2023**, *14*, 5410.
[114] X. Zhang, J. Yu, C. Zhao, Y. Si, *ACS Nano* **2023**, *17*, 21813.
[115] H. Liu, X. Zhang, Y. Liao, J. Yu, Y. T. Liu, B. Ding, *Adv. Mater.* **2024**, *36*, 2313720.
[116] X. Chang, Y. Yang, X. Cheng, X. Yin, J. Yu, Y. T. Liu, B. Ding, *Adv. Mater.* **2024**, *36*, 2406055.
[117] J. Lin, B. Ding, J. Yang, J. Yu, G. Sun, *Nanoscale* **2012**, *4*, 176.
[118] H. Wu, Y. Li, L. Zhao, S. Wang, Y. Tian, Y. Si, J. Yu, B. Ding, *ACS Appl. Mater. Interfaces* **2020**, *12*, 27562.
[119] Y. Tian, Y. Chen, S. Wang, X. Wang, J. Yu, S. Zhang, B. Ding, *Adv. Funct. Mater.* **2025**, *35*, 2414229.
[120] X. Cheng, X. Chang, X. Zhang, J. Dai, H. Fong, J. Yu, Y. T. Liu, B. Ding, *Adv. Mater.* **2024**, *36*, 2307690.
[121] L. Su, M. Li, H. Wang, M. Niu, D. Lu, Z. Cai, *ACS Appl. Mater. Interfaces* **2019**, *11*, 15795.
[122] X. Zhang, F. Wang, L. Dou, X. Cheng, Y. Si, J. Yu, B. Ding, *ACS Nano* **2020**, *14*, 15616.
[123] X. Zhang, X. Cheng, Y. Si, J. Yu, B. Ding, *ACS Nano* **2022**, *16*, 5487.
[124] W. Li, Y. Jiang, H. Liu, C. Wang, X. Zhou, S. Jiang, Y. Mu, L. Wang, X. He, M. Li, *ACS Appl. Mater. Interfaces* **2023**, *15*, 46010.
[125] M. Hua, S. Wu, Y. Ma, Y. Zhao, Z. Chen, I. Frenkel, J. Strzalka, H. Zhou, X. Zhu, X. He, *Nature* **2021**, *590*, 594.
[126] X. Zhang, J. Yu, Y. Si, *Adv. Mater.* **2025**, *37*, 2412962.
[127] H. Wang, X. Zhang, N. Wang, Y. Li, X. Feng, Y. Huang, C. Zhao, Z. Liu, M. Fang, G. Ou, H. Gao, X. Li, H. Wu, *Sci. Adv.* **2017**, *3*, 1603170.

[128] L. Cao, Q. Liu, J. Ren, W. Chen, Y. Pei, D. L. Kaplan, S. Ling, *Adv. Mater.* **2021**, *33*, 2102500.
[129] Z. Li, Z. Cui, L. Zhao, N. Hussain, Y. Zhao, C. Yang, X. Jiang, L. Li, J. Song, B. Zhang, Z. Cheng, H. Wu, *Sci. Adv.* **2022**, *8*, abn3690.
[130] K. Huang, F. Liang, J. Sun, Q. Zhang, Z. Li, S. Cheng, W. Li, H. Yuan, R. Liu, Y. Ge, Y. Cheng, K. Wang, J. Jiang, Y. Yang, M. Ma, F. Yang, C. Tu, Q. Xie, W. Yin, X. Wang, Y. Qi, Z. Liu, *Adv. Mater.* **2024**, *36*, 2313752.
[131] S. Chen, D. Xu, H. Yin, R. Huang, W. Qi, R. Su, K. Zhang, *Small* **2024**, *20*, 2401283.
[132] X. Gong, X. Yin, F. Wang, X. Liu, J. Yu, S. Zhang, B. Ding, *Small* **2023**, *19*, 2205067.
[133] https://www.grandviewresearch.com/industry-analysis/winter-wear-market (accessed: April 2025).
[134] J. Li, X. Hu, Y. Pan, J. Qian, Z. Qiang, Z. Meng, C. Ye, M. Zhu, *Adv. Funct. Mater.* **2024**, *34*, 2410940.
[135] X. Li, G. Dong, Z. Liu, X. Zhang, *ACS Nano* **2021**, *15*, 4759.
[136] D. Wang, Y. Peng, J. Dong, L. Pu, K. Chang, X. Yan, H. Qian, L. Li, Y. Huang, T. Liu, *Compos. Commun.* **2023**, *37*, 101429.
[137] S. Wang, C. Zhu, F. Wang, J. Yu, S. Zhang, B. Ding, *Small* **2023**, *19*, 2302835.
[138] S. Wang, X. Zhao, Z. Yang, R. Ding, Y. Tian, X. Wang, J. Yu, S. Zhang, B. Ding, *Adv. Funct. Mater.* **2024**, *34*, 2316657.
[139] W. Zhang, G. Liang, S. Wang, F. Yang, X. Liu, J. Yu, S. Zhang, B. Ding, *Adv. Funct. Mater.* **2024**, *35*, 2412424.
[140] Y. Yu, C. Xu, Z. Hu, H. Xiang, J. Zhang, X. Zhang, Y. Cheng, L. Zhu, M. Zhu, *Adv. Mater.* **2024**, *36*, 2414731.
[141] X. Zhang, W. Huang, J. Yu, C. Zhao, Y. Si, *Adv. Funct. Mater.* **2025**, *35*, 2416857.
[142] Z. Xu, Y. Liu, Q. Xin, J. Dai, J. Yu, L. Cheng, Y. T. Liu, B. Ding, *Adv. Mater.* **2024**, *36*, 2401299.
[143] X. Feng, M. Ouyang, X. Liu, L. Lu, Y. Xia, X. He, *Energy Storage Mater.* **2018**, *10*, 246.
[144] Q. Wang, B. Mao, S. I. Stoliarov, J. Sun, *Prog. Energy Combust. Sci.* **2019**, *73*, 95.
[145] Y. Xiao, M. Yan, L. Shi, L. Gong, X. Cheng, H. Zhang, Y. Pan, *Energy Storage Mater.* **2023**, *61*, 102871.
[146] X. Xu, Q. Zhang, M. Hao, Y. Hu, Z. Lin, L. Peng, T. Wang, X. Ren, C. Wang, Z. Zhao, C. Wan, H. Fei, L. Wang, J. Zhu, H. Sun, W. Chen, T. Du, B. Deng, G. J. Cheng, I. Shakir, C. Dames, T. S. Fisher, X. Zhang, H. Li, Y. Huang, X. Duan, *Science* **2019**, *363*, 723.
[147] Y. Feng, Y. Guo, X. Li, L. Zhang, J. Yan, *ACS Nano* **2024**, *18*, 19054.
[148] T. Ren, Z. Chen, J. Chen, X. Huang, X. Li, J. Zhang, Q. Lu, C. T. Hung, T. Zhao, M. Wang, D. Zhao, *Small* **2025**, *21*, 2410872.
[149] X. Zhang, J. Zhou, K. Wu, S. Zhang, L. Xie, X. Gong, L. He, Y. Ni, *Adv. Mater.* **2024**, *36*, 2311817.
[150] H. Dong, S. Wei, W. Chen, B. Lu, Z. Cai, B. Yang, X. Li, X. Li, *ACS Nano* **2025**, *19*, 11712.
[151] B. Zhao, Y. Wang, H. Huang, *Ceram. Int.* **2024**, *50*, 18510.
[152] Y. Duan, L. Guan, Z. Min, R. Fu, J. Li, L. Fan, H. Abadikhah, B. Zhao, B. Dong, R. Zhang, *Adv. Eng. Mater.* **2024**, *26*, 2401649.
[153] P. Soltani, M. Azimian, A. Wiegmann, M. Zarrebini, *J. Sound Vib.* **2018**, *426*, 1.
[154] D. Zong, L. Cao, X. Yin, Y. Si, S. Zhang, J. Yu, B. Ding, *Nat. Commun.* **2021**, *12*, 6599.
[155] T. Xue, S. Yuan, Y. Yang, X. Wan, Y. Yang, X. Mu, L. Zhang, C. Zhang, W. Fan, T. Liu, *Adv. Funct. Mater.* **2025**, *35*, 2417734.
[156] Y. Cheng, B. Ma, P. Hu, J. Zhang, D. Hu, J. Wang, *Adv. Funct. Mater.* **2023**, *33*, 2309148.

Xiaobao Gong earned his Ph.D. from Donghua University. Currently, he is a Postdoctoral Fellow in the School of Fashion and Textiles, Hong Kong Polytechnic University (PolyU). His research focuses on micro/nanofiber materials and functional textiles.

Jianming Chen obtained a Ph.D. from the Hong Kong Polytechnic University. He is currently a Research Assistant Professor in the School of Fashion and Textiles at PolyU. Dr. Chen's research is mainly focused on fibrous materials and functional polymers.

Xungai Wang received his Ph.D. from the University of New South Wales (UNSW). He is currently a Global STEM Scholar and the Chair Professor of Fiber Science and Technology in the School of Fashion and Textiles at PolyU. He also serves as Director of the Joint Research Centre for Fiber Innovations and Renewable Materials (JRC-FIRM). His research is mainly focused on sustainable and functional fibers and textiles.